Title

Assessing the Biosynthetic Inventory of the Biocontrol Fungus *Trichoderma afroharzianum* T22.

Journal

Journal of agricultural and food chemistry, 71(30)

ISSN

0021-8561

Authors

Han, Wenyu
Wu, Zhongshou
Zhong, Zhenhui
et al.

Publication Date

2023-08-01

DOI

10.1021/acs.jafc.3c03240

Assessing the Biosynthetic Inventory of the Biocontrol Fungus *Trichoderma afroharzianum* T22

Wenyu Han[1], Zhongshou Wu[3,4], Zhenhui Zhong[3,4], Jason Williams[1], Steven E. Jacobsen[3,4,5,6], Zuodong Sun[2]* and Yi Tang[1,2]*

1. Department of Chemistry and Biochemistry, University of California, Los Angeles, California 90095, United States

2. Department of Chemical and Biomolecular Engineering, University of California, Los Angeles, California 90095, United States

3. Department of Molecular Cell and Developmental Biology, University of California, Los Angeles, California 90095, United States

4. Howard Hughes Medical Institute, University of California, Los Angeles, California 90095, United States

5. Eli & Edythe Broad Center of Regenerative Medicine & Stem Cell Research, University of California, Los Angeles, California 90095, United States

6. Department of Biological Chemistry, University of California, Los Angeles, California 90095, United States

* Emails of corresponding authors: zsun12@ucla.edu; yitang@ucla.edu

Abstract

Natural products biosynthesized from biocontrol fungi in the rhizosphere can have both beneficial and deleterious effects on plants. Herein, we performed a comprehensive analysis of natural product biosynthetic gene clusters (BGCs) from a widely used biocontrol fungus *Trichoderma afroharzianum* T22 (ThT22). This fungus encodes at least 64 BGCs, yet only seven compounds and four BGCs were previously characterized or mined. We correlated 21 BGCs of ThT22 with known primary and secondary

metabolites through homologous BGC comparison; and characterized one unknown BGC involved in the biosynthesis of eujavanicol A using heterologous expression. In addition, we performed untargeted transcriptomics and metabolic analysis to demonstrate activation of silent ThT22 BGCs via the "one strain many compound" (OSMAC) approach. Collectively, our analysis showcases the biosynthetic capacity of ThT22 and paves the way for fully exploring the roles of natural products of ThT22.

Keywords

Biocontrol and biofertilizer fungi, secondary metabolite, natural product, biosynthesis, transcriptomics, OSMAC

1. Introduction

Global food security faces increasing challenges from a growing population, climate change and crop losses due to plant pests and pathogens.[1,2] Therefore, effective and ecofriendly methods that can promote plant growth and combat plant diseases are much needed. Certain fungal species, particularly those in the *Trichoderma* genus, have long been utilized as biofertilizers and biocontrol agents for such purposes.[3] A prime representative is *Trichoderma afroharzianum* T22 (formerly *Trichoderma harzianum* T22,[4] designated as ThT22 in this work), one of the most widely used biofertilizer fungi in agricultural applications.[5] ThT22 can colonize plant rhizosphere and increase plant robustness by a variety of mechanisms including mycoparasitism and antibiosis,[6] nutrient sequestration,[7] boosting immunity,[8] and promoting root growth and development.[9] It is proposed that numerous beneficial *Trichoderma*-plant interactions are mediated by fungal secondary metabolites.[10] Also known as natural products, these small molecular weight compounds can act as plant hormones to regulate plant growth or as fungicides to kill plant pathogens[11,12]. As synthetic pesticides have become less effective due to the rise of resistance, combined with increased environmental concerns from the public and regulatory agencies, natural products remain an important source for developing safe methods to promote plant fitness.[13]

Fully harnessing the agricultural benefits of the *Trichoderma* species such as ThT22 requires (1) a complete catalog of the secondary metabolome of the biocontrol species; and (2) a deep understanding of their biological roles, both beneficial and deleterious to the plant and other microbes in the rhizosphere. While ~ 400 compounds have been reported from *Trichoderma*,[14] a vast majority of these are isolated from strains not registered as biocontrol agents.[15] On the other hand, only four compounds (not double counting structurally related ones) have been directly isolated from ThT22 (Figure 1A).[12,16,17] These compounds represent only a fraction of natural products that can be produced based on analysis of the biosynthetic gene clusters (BGCs) of ThT22.[18] This is a widely observed phenomenon as most BGCs in fungi are cryptic or silent under axenic culturing conditions in the laboratory.[19] Mining these unassigned BGCs using various approaches, including transcriptional activation in native host, or heterologous expression in model fungi, has been fruitful in discovering both known or novel natural products.[19–21] Two previously unknown compounds, trihazone, and tricholignan A, were identified from ThT22 starting from their respective BGCs (Figure 1B).[18,22] Tricholignan A was shown to be a redox-active ortho-hydroquinone that can facilitate reductive iron assimilation and rescue plant chlorosis under iron deficient conditions.[18] Such example illustrates the untapped natural product biosynthetic potential of ThT22, as well as unexplored roles of these compounds in plant-fungi interactions.

To aid the discovery of both known and novel natural products from ThT22, we performed a comprehensive evaluation of the BGC inventory of ThT22. We analyzed all 64 BGCs predicted to be encoded by this species and associated 22 of them with reported natural products via bioinformatics and heterologous expression. Combining these with four previously characterized BGCs, we can now associate ~ 40% of the predicted biosynthetic capacity of ThT22 with known natural products. In addition, we examined the impact of culturing conditions on the secondary metabolome of ThT22 via untargeted transcriptomics and metabolic analysis. Using this approach, we demonstrated that a number of ThT22 BGCs can be activated at both transcription and metabolite level. Our results set the foundation

of exploring the remaining 38 unknown BGCs in ThT22, and mapping of their roles in plant-ThT22 interactions.

2. Materials and Methods

2.1. Bioinformatics

The genome of ThT22 was downloaded from the Joint Genome Institute (JGI) Genome Portal[23] and analyzed by AntiSMASH fungal version 5.1.0 for global prediction of BGCs.[24] The detection strictness of AntiSMASH was set to "loose" to obtain as many predictions as possible. The genes in predicted BGCs were further annotated by 2ndfind.[25] Homologous proteins were searched using NCBI BLAST.

2.2. Genomic DNA extraction from ThT22

ThT22 was obtained from the American Type Culture Collection (ATCC 20847) and maintained on potato dextrose agar (Sigma). A 10 mL culture of ThT22 in potato dextrose broth (Sigma) was shaken for 7 days at 28 °C and 250 rpm. Genomic DNA was then extracted from fungal cell body with Quick-DNA™ Fungal/Bacterial Miniprep Kit (Zymo research) following the manufacturer's protocol. In brief, lyophilized fungal body was lysed by beating with beads, and pure genomic DNA was acquired through column purification and elution.

2.3. General DNA manipulation techniques

Plasmids used for heterologous expression of eujavanicol A (cluster 5 in Table 1) were constructed via homologous recombination in *Saccharomyces cerevisiae* YJB80 as previously described.[26] All primers used in this study are listed in Supporting Information Table S1.

2.4. Heterologous reconstitution of the eujavanicol A BGC (cluster 5)

Aspergillus nidulans ΔEMΔST[27] was transformed with plasmids containing genes from cluster 5 by a previously reported protocol.[26] The resulting transformants were grown on CD-Agar and metabolites were extracted as previously described.[26] Metabolic profile analysis was performed with a Shimadzu 2020

EV LC-MS with a reverse-phase column (Phenomenex Kinetex, C18, 1.7 µm, 100 Å, 2.1 × 100 mm). The solvent program was a linear gradient of 5-95% water-acetonitrile (containing 0.1% formic acid) in 15 minutes at 0.3 mL/min^{-1}.

2.5. Compound isolation and characterization

A. nidulans transformed with plasmids harboring EujABCDE were grown on 80 × 50 mL CDST[26] agar plates at 28 °C for 5 days. The agar plates were then cut into pieces and sonicated in 4 L of 3:1 ethyl acetate/acetone mixture for 1 hour. The agar pieces were removed by filtration and extracted again with 4 L of 3:1 ethyl acetate/acetone. The two extractions were combined and evaporated to dryness by a rotary evaporator. The crude extracts were then separated by silica flash chromatography with a CombiFlash® system and a gradient of hexane and ethyl acetate. The targeted compounds were further purified by an UltiMate™ 3000 Semi-Preparative HPLC (ThermoFisher) with an Eclipse XDB-C18 column (5 µm, 9.4 × 250 mm, Agilent) and an isocratic gradient of 55% acetonitrile-water (containing 0.1% formic acid) to yield 1 g of pure eujavanicol A as white gel-like solids (250 mg/L culture). Accurate masses of purified eujavanicol A were measured by an Agilent 1260 Infinity II LC equipped with an InfinityLab Poroshell 120 EC-C18 column (2.7 µm, 3.0 × 50 mm) and a 6545 qTOF high resolution mass spectrometer (UCLA Molecular Instrumentation Center). NMR spectra were recorded on a Bruker AV500 NMR spectrometer with a 5 mm dual cryoprobe (500 MHz, UCLA Molecular Instrumentation Center).

Eujavanicol A: 1H NMR ($CDCl_3$, 500 MHz) δ 5.96 (1H, dt, H-4), 5.65 (1H, ddd, H-3), 3.98 (1H, q, H-6), 3.90 (1H, m, H-11), 3.83 (1H, m, H-11), 3.37 (1H, dd, H-5), 2.82 (1H, ddd, H-10), 2.63 (1H, ddd, H-10), 2.08 (1H, tq, H-4a), 1.90 (1H, m, H-2), 1.88 (1H, t, H-8a), 1.79 (1H, dt, H-7eq), 1.68 (1H, m, H-8), 1.48 (1H, m, H-7ax), 1.42 (1H, m, H-2′), 1.20 (3H, s, Me-1), 1.07 (1H, m, H-1′), 0.89 (3H, d, Me-1′), 0.76 (3H, m, H-3′), 0.76 (1H, m, H-2′), 0.54 (3H, d, Me- 8); 13C NMR ($CDCl_3$, 125 MHz) δ 215.7 (C-9), 126.3 (C-4), 123.8 (C-3), 75.3 (C-5), 69.6 (C-6), 57.8 (C-11), 52.6 (C-1), 52.3 (C-2), 43.1 (C-8a), 41.3 (C-7), 41.2 (C-10), 39.0 (C-4a), 37.2 (C-1′), 30.6 (C-8), 24.4 (C-2′), 22.4 (Me-8), 19.4 (Me-1), 19.2 (Me-1′), 12.6 (C-3′). HRMS 325.2373 (M+H, calculated for $C_{19}H_{32}O_4$: 325.2360, deviation 4.1 ppm).

2.6. Untargeted transcriptomics and metabolic analysis of ThT22 on different media

ThT22 was cultured on six different media at 28 °C for 7 days: CD (1% glucose, 5% nitrate salt mix (0.12 g/mL $NaNO_3$, 0.104 g/mL KCl, 0.104 g/mL $MgSO_4 \cdot 7H_2O$, 0.304 g/mL KH_2PO_4), 0.1% trace element mix (0.022 g/mL $ZnSO_4 \cdot 7H_2O$, 0.011 g/mL H_3BO_3, 0.005 g/mL $MnCl_2 \cdot 4H_2O$, 0.0016 g/mL $FeSO_4 \cdot 7H_2O$, 0.0016 g/mL $CoCl_2 \cdot 5H_2O$, 0.0016 g/mL $CuSO_4 \cdot 5H_2O$, 0.0011 g/mL $(NH_4)_6Mo_7O_{24} \cdot 4H_2O$, pH 6.5), 2% agar); CGN (corn steep liquor (Sigma) 15 g/L, glucose 30 g/L, $NaNO_3$ 2 g/L, $CaCO_3$ 7 g/L, agar 15 g/L); MMK2 (mannitol 40 g/L, yeast extract 5 g/L, Murashige & Skoog Salts (Sigma) 4.3 g/L, agar 20 g/L); PDA (Sigma); V8 (V8 juice 200 mL/L, $CaCO_3$ 2 g/L, agar 15 g/L); SSC (glucose 1%, modified starch 6%, cottonseed flour 1%, soybean flour 1%, KH_2PO_4 1.6%, Na_2HPO_4. $12H_2O$ 1.2%,). Triplicates were performed for each medium. Metabolites were extracted and analyzed by the Agilent LC-qTOF as described above.

Fungal mycelia were collected from the agar plates and total RNA was extracted by Zymo Direct-zol RNA MiniPrep Kit (Zymo Research). A total of 1 μg of total RNA was used for library preparation with TruSeq Stranded mRNA kit (Illumina). Libraries were sequenced on NovaSeq 6000 (Illumina). Reads were aligned to the reference genome ThT22 by Bowtie2[28] (v2.1.0) and expression abundance was calculated using RSEM[29] with default parameters. The R package pheatmap[30] was used to visualize the results.

3. Results

3.1. Global annotation of ThT22 BGCs

We obtained the sequenced genome data from JGI Genome portal[23] and predicted BGCs encoding known core enzymes using AntiSMASH.[24] The analysis identified 64 putative BGCs (Table 1, Supporting Information Figure S1). This number is significantly larger than the average number of BGCs (~40) encoded by well-studied fungal taxon Pezizomycotina (which contains *Aspergillus, Penicillium*, as well as *Trichoderma*), suggesting that ThT22 is among the most prolific producers of fungal natural products.[31]

Based on the core enzyme encoded in each cluster, these 64 BGCs can be grouped into six families that cover all major classes of fungal natural products (Figure 1C). There are 19 BGCs encoding polyketide synthases (PKSs), 23 encoding non-ribosomal peptide synthetases (NRPSs), 11 encoding terpene synthases/cyclases, five encoding PKS-NRPS hybrid megasynthetases, one encoding enzymes for biosynthesis of ribosomally synthesized and post translationally modified peptides (RiPPs), and five encoding NRPSs producing lipopeptides (NRPS with *N*-terminal condensation domain). The result suggests that ThT22 should be able to synthesize 64 natural products at a minimum, yet only seven compounds (four isolated, three genome-mined) are known from the organism (Figure 1A and 1B). Four of these seven compounds have associated BGCs (designated by (C) in Table 1): tricholignan A (cluster 10),[18] dichlorodiaporthin (cluster 15),[32] harzianic acid (cluster 42),[12] and trihazone (cluster 47).[22] Hence, at the onset of this study, 60 of the 64 predicted BGCs have not been associated with any natural products. . **3.2. Identification of ThT22 BGCs homologous to characterized biosynthetic pathways**

Homologous BGCs that biosynthesize the same or closely related natural product are often found in multiple fungal species. Therefore, a portion of the 60 unassigned BGCs can be dereplicated bioinformatically and linked to known metabolites. To do so, we first searched for characterized proteins that share at least 45% sequence identity with core genes from the unassigned ThT22 BGCs. We then compared characterized biosynthetic pathways containing the hits to the corresponding ThT22 BGCs. A homologous BGC is designated when *all* essential proteins for biosynthesis are conserved, and the sequence identity of all homologous proteins between two species are at least 45%. Using this analysis, we can dereplicate 21 of the 60 unassigned ThT22 BGCs as shown below (Figure 1D, (P) in Table 1).

3.2.1 PKS-containing BGCs (Figure 2)

Cluster 1-Tv6-931

Cluster 1 contains a highly reducing PKS (HRPKS) (JGI protein ID: 605427) sharing 91% identity with Tv6-931 from *Trichoderma virens* (Figure 2A).[33] Tv6-931 is a noncanonical HRPKS with a *C*-terminal carnitine acetyltransferase (CAT) domain. When assayed *in vitro*, this CAT domain releases

the polyketide product of Tv6-931 from its ACP domain by transesterification with polyalcohols such as glycerol to produce compounds **1** and **2**. However, the physiological substrate of the CAT and the true product of Tv6-931 remain unresolved. There are additional homologous genes of unknown function such as a nitroreductase (JGI protein ID: 584977) and a DUF469 protein (JGI protein ID: 2149).

Cluster 7-unidentified fungal conidial pigment:

The core gene in Cluster 7 is a nonreducing PKS (NRPKS) (JGI protein ID: 624619) sharing 76% identity with PKS1 from *Metarhizium anisopliae* (Figure 2B).[34] PKS1 is involved in the biosynthesis of a structurally uncharacterized fungal conidial pigment. The remaining genes in the cluster include a EthD family dehydratase (JGI protein ID: 353081) and a laccase (JGI protein ID: 523541) which are also conserved in fungal pigment BGCs.[35]

Cluster 8-trichoxide:

Cluster 8 encodes 12 enzymes, all of which share high identity with the trichoxide (**3** in Figure 2C) biosynthetic enzymes VirA-L from *T. virens.*[36] In the trichoxide pathway, the core HRPKS VirA (homologous to JGI protein ID: 615175) produces the aldehyde **4** via reductive release by possibly the cupin domain containing protein VirC (homologous to JGI protein ID: 928684). Successive oxidation of hydroxy groups in **4** by short-chain dehydrogenase/reductase (SDR) enzymes VirB (homologous to JGI protein ID: 928684) and VirD (homologous to JGI protein ID: 453581) produce compound **5** which can undergo aldol-cyclization and aromatization to form hydroxy benzaldehyde **6**. A series of late-stage redox transformations by the remaining *vir* enzymes generate the epoxyquinone moiety of **3**. Both **3** and **6** exhibited antifungal activities against *Saccharomyces cerevisiae* and *Candida albicans.*[36] Compound **6** also inhibits growth of *Staphylococcus aureus* and *Bacillus subtilis.*

Cluster 12-t22 azaphilone:

Cluster 12 shares high identity with the *aza* cluster in *Trichoderma guizhouense* which is responsible for the biosynthesis of a group of azaphilones including t22 azaphilone (**7** in Figure 2D).[37] Compound **7** is a major metabolite from ThT22 and displays marked *in vitro* inhibitory activity against

plant pathogens such as *Rhizoctonia solani*, *Pythium ultimum,* and *Gaeumannomyces graminis* var. *tritici*.[16] Although the *aza* cluster has not been characterized in detail, gene disruption experiments[37] and analysis of characterized pathways of related compounds enabled us to propose the following pathway for **7** (Figure 2D). HRPKS (JGI protein ID: 621517) and NRPKS (JGI protein ID: 558993), which are homologous to Aza1 and Aza2, respectively, function in tandem to produce benzaldehyde **8**. Flavin dependent monooxygenase (FMO) (JGI protein ID: 293506) homologous to Aza9 then hydroxylates **8**, which initiates a series of reactions including keto-enol tautomerization, cyclization, and dehydration to form the bicyclic pyran **9**.[38] Acetyltransferase (JGI protein ID: 589621) homologous to Aza10 is then proposed to acylate **9** with β-hydroxybutyryl-CoA (a primary metabolite) to form **7**. There are three remaining uncharacterized enzymes in the cluster that have close homologues in the *aza* BGC: SnoaL like NTF2 family protein (JGI protein ID: 503145), dehydratase (JGI protein ID: 599745), and FMO (JGI protein ID: 532797).

Cluster 18-chrysophanol/pachybasin:

Cluster 18 encodes 17 biosynthetic enzymes, seven of which are homologous to reported chrysophanol biosynthetic genes (Figure 2E).[39] The anthraquinones chrysophanol (**13**) and pachybasin (**10**) are both major metabolites of ThT22[16] and have diverse biological functions including anti-inflammatory activities and cytotoxicity.[40,41] Both compounds were structurally characterized by MicroED analysis directly from ThT22 extracts.[42] NRPKS (JGI protein ID: 195120) and thioesterase (TE) (JGI protein ID: 635129), which are homologous to NsrB and NsrC, respectively, are proposed to biosynthesize atrochrysone carboxylic acid (**11**), which then undergoes decarboxylation catalyzed by NTF2 family protein (JGI protein ID: 519738) that is homologous to NsrE, and oxidation catalyzed by anthrone oxygenase (JGI protein ID: 195056) homologous to NsrD, to form the anthraquinone emodin (**12**). A three-enzyme cascade consists of two SDRs (JGI protein ID: 507580 and 624766) and an EthD family dehydratase (JGI protein ID: 536449), all with close homologues in the characterized chrysophanol pathway, then are proposed to convert emodin to **13**. Given the high structural similarity

between chrysophanol and pachybasin, it is proposed that the two compounds share the same biosynthetic pathway. Since cluster 18 is the only cluster in ThT22 encoding anthraquinone biosynthetic genes, we propose that the remaining enzymes encoded in this cluster are responsible for the biosynthesis of pachybasin (**10**).

3.2.2 NRPS-containing BGCs (Figure 3)

Cluster 20-destruxin:

Cluster 20 encodes three enzymes, a six-module NRPS (JGI protein ID: 626604), a P450 (JGI protein ID: 488926), and a reductase (JGI protein ID: 488922) that share 53%, 60%, 58% sequence identity with characterized destruxin biosynthetic enzymes DtxS1, DtxS2 and DtxS3, respectively (Figure 3A).[43] Destruxins are vacuolar-type ATPase (V-ATPase) inhibitors and have been explored for use as anticancer and insecticidal agents.[44] The domain arrangement in the NRPS is the same as that found in DtxS1 that produces destruxin B (**14**): ATC-ATEC-ATC-ATC-A(*N*-MT)TC-A(*N*-MT)TC. The P450 homologous to DtxS2 likely modifies destruxin B into different destruxin derivatives. The reductase homologous to DtxS3 is likely responsible for the biosynthesis of α-hydroxyisocaproic acid (**15**) which is a building block of **14.** The destruxin BGC from *Metarhizium robertsii* encodes DtxS4, which is a PLP-dependent aminotransferase that converts aspartic acid into β-alanine (**16**), also a building block of **14**. In ThT22, the homolog (JGI protein ID: 594801) of DtxS4 (57% identical), is not clustered with the rest of the biosynthetic enzymes.

Cluster 21-11'-deoxyverticillin A:

The NRPS-encoding cluster 21 is homologous to the *ver* BGC from *Clonostachys rogersoniana* that is found to be responsible for biosynthesis of epipolythiodioxopiperazine (ETP) 11′-deoxyverticillin A (**17** in Figure 3B).[45] This compound and structurally related verticillin A have potent cytotoxicity against HCT-116 human colon carcinoma.[46]. Gene disruption experiments showed that most enzymes in the *ver* BGC are required for verticillin production, but the pathway remains biochemically uncharacterized.[45] Based on the biosynthesis of well-studied ETP gliotoxin, we proposed the following

roles for enzymes in cluster 21.[47] The NRPS (JGI protein ID: 447208) homologous to VerP may synthesize the D-Ala-D-Trp diketopiperazine scaffold **18**. Four enzymes (JGI protein IDs: 626725, 415095, 476805, and 595190) with homologues in the *ver* pathway collectively catalyze glutathione mediated C_α-sulfurization of **18** to afford **19**. One of the four enzymes (JGI protein ID: 415095) is a fused protein consists of homologues of VerG and VerJ. Compound **19** may undergo thiol oxidation and *N*-methylation catalyzed by homologues of VerN (JGI protein ID: 489305) and VerT (JGI protein ID: 613487), respectively, to form **20**. The P450 (JGI protein ID: 547922) is a homologue of VerB, which shares 25% identify with DesC that catalyzes aryl-coupling to form the bicoumarin desertorin, and therefore may catalyze the dimerization of **20** to form **21**.[48] The remaining P450 (JGI protein ID: 595181) may catalyze the final hydroxylation of **21** to produce 11′-deoxyverticillin A.

Cluster 24-ferricrocin:

Cluster 24 encodes four conserved enzymes, an NRPS (JGI protein ID: 211076), L-ornithine-N_5-monooxygenase (JGI protein ID: 210889), betaine aldehyde dehydrogenase (JGI protein ID: 210847) and choline oxidase (JGI protein ID: 476913) (Figure 3C). The NRPS shares 52 % identity with ferricrocin (**22**) synthetase NRPS 2 from *Fusarium graminearum.*[49] Both NRPSs have identical domain architecture of A-T-C-A-T-C-T-C-A-T-C-T-C-T-C. The L-ornithine-N_5-monooxygenase is proposed to catalyze the first step in the biosynthesis of all hydroxamate-containing siderophores such as ferrichrome. Although an acetyltransferase homologous to SidL found in ferricrocin biosynthesis in *Aspergillus fumigatus* is not conserved in cluster 24, an unclustered homologue (JGI protein ID: 553276) with 55% sequence identity is encoded elsewhere in the genome.

Cluster 25-choline:

Cluster 25 encodes a single NRPS-like protein (JGI protein ID: 291737) with a domain architecture of A-T-R-R (Figure 3D). This enzyme shares 68% activity with characterized glycine betaine (**24** in Figure 3D) reductase ATRR from *Aspergillus nidulans.*[50] Similar to the characterized enzyme, the A domain of 291737 may activate glycine betaine with ATP and load onto the T domain as a thioester.

The two R domains then perform consecutive two-electron reduction of the thioester into choline (**23**). This pathway is proposed to be an alternative choline biosynthetic pathway in fungi and maintains homeostatic levels of glycine betaine in the cell.[50] While this enzyme is involved in primary metabolism of the host, we are including it in this work since the NRPS is recognized by AntiSMASH in BGC predictions.

Cluster 32-fumicicolin A:

The core gene of cluster 32 encodes a single module NRPS (JGI protein ID: 531123) that shares 71% identity to CrmA from *A. fumigatus* (Figure 3E).[51] The domain arrangement of this NRPS is unusual: an *N*-terminal isocyanide synthase (ICS) domain followed by adenylation, thiolation and transferase domains. Four metabolites have been associated with CrmA: fumicicolin A (**25**), isocyanovaline (**26**), *N*-formylvaline (**27**), and fumivaline A. The first product of CrmA and homologues is most likely **26**, which may be hydrolyzed nonenzymatically to produce **27**. This compound is then esterified with D-mannitol to afford **25**. In addition, **27** is also incorporated into the ergot alkaloid biosynthesis pathway in *A. fumigatus* to produce fumivaline A.[51] Two other conserved proteins CrmB and CrmD, of which homologues are present in cluster 32, are not required to produce compounds **25-27** and their functions remain obscure.[51] Fumicicolin A has been proposed to act as a phytotoxin, such as the structurally related brassicicolin A, to induce necrosis of plant tissues and enable its fungal producer to obtain copper from the host plant under copper-starved conditions.[51]

Cluster 35-fusarinine-like siderophore:

Cluster 35 encodes a two-module NRPS (JGI protein ID: 323124) that shares 42% identity to SidD from *Aspergillus fumigatus* A1163 (Figure 3F).[52] SidD is part of a six-gene pathway to produce triacetylfusarinine C (**28**). While cluster 35 also encodes homologs of SidI (CoA-ligase, JGI protein ID: 560985) and SidF (acyltransferase, JGI protein ID: 600537)., three remaining homologous genes (SidA, SidH, and SidG) are found elsewhere in ThT22 genome. Therefore, the product of cluster 35 is likely triacetylfusarinine C or a structurally similar siderophore.

Cluster 39- L-2-aminoadipate-δ-semialdehyde (primary metabolism):

Cluster 39 identified by AntiSMASH encodes a single enzyme (JGI protein ID: 544585) that shares 51% identity to the large subunit of L-2-aminoadipate reductase Lys2 from *Penicillium chrysogenum.*[53] This is a well-characterized single module NRPS (A-T-R) and is part of the lysine biosynthetic pathway that reduces L-2-aminoadipate to L-2-aminoadipate-δ-semialdehyde. (Figure 3G)

3.2.3 Terpene-Cyclase containing BGCs (Figure 4)

Cluster 46-trichobrasilenol:

Cluster 46 encodes a sesquiterpene cyclase (JGI protein ID: 210618) that is 73% identical to trichobrasilenol (**29**) synthase TaTC6 from *Trichoderma atroviride* (Figure 4A).[54] The only other conserved enzyme is an *O*-glycosyltransferase (JGI protein ID: 489462), which may transfer a sugar moiety to **29** to form a glycosylated terpene product.

Cluster 47-trichoacorenol:

The core gene of Cluster 47 encodes a sesquiterpene cyclase (JGI protein ID: 291000) that shares 74% identity to trichoacorenol (**30**) synthase NsTAS from *Nectria sp.* (Figure 4B).[55] This cluster has one additional conserved protein (JGI protein ID: 290978) which is predicted to be a heterokaryon incompatibility protein and is unlikely to be biosynthetic.

Cluster 51-squalene (primary metabolism):

Cluster 51 encodes a predicted squalene cyclase (JGI protein ID: 578267) which shares 57% identity to squalene synthase ERG9 from *A. fumigatus.*[56] Being the only predicted squalene synthase in the genome, this protein is most likely part of primary metabolism in which squalene is produced as a precusor to sterols.

Cluster 52-tricinoloniol acid:

Cluster 52 encodes a sesquiterpene cyclase (JGI protein ID: 461327) which is 81% identical to TraA from *Trichoderma hypoxylon* (Figure 4C).[57] Deletion of TraA in *T. hypoxylon* abolished production of tricinoloniol acids A-C (**31-33**). Other enzymes proposed to be involved in the biosynthesis are not

clustered with TraA in the reported host. No other biosynthetic enzymes are found near this terpene cyclase in ThT22.

Cluster 54-sordarin:

Cluster 54 shares high sequence identity with the *sdn* BGC from *Sordaria araneosa* that is characterized to be responsible for the biosynthesis of the antifungal sordarin (**34** in Figure 4D), which is a potent inhibitor of fungal elongation factor 2.[26,58,59] The predicted terpene cyclase (JGI protein ID: 593170) is highly homologous to SdnA that synthesizes the 5-8-5 tricyclic cycloaraneosane from geranylgeranyl pyrophosphate (GGPP). This tricyclic hydrocarbon can be morphed into a highly reactive intermediate **35** via four steps catalyzed by three P450s that are conserved between cluster 54 and the *sdn* BGC: dihydroxylation (JGI protein ID: 471077), desaturation (JGI protein ID: 568624), diol cleavage (JGI protein ID: 471077, second function), and aldehyde oxidation (JGI protein ID: 582974). Compound **35** then undergoes intramolecular Diels-Alder (IMDA) reaction to form **36**, which is then monohydroxylated by a fourth P450 (JGI protein ID:568618) to form sordaricin **37**. The IMDA reaction was shown to be accelerated by a NTF2 family enzyme SdnG (homologues is JGI protein ID: 611681).[26] Glycosyltransferase (JGI protein ID: 568626) completes the biosynthesis of sordarin by glycosylating **37** with sordarose **38,** which may be biosynthesized from GDP-D-mannose by conserved SDR (JGI protein ID: 633857), dehydrogenase (JGI protein ID: 582978) and methyltransferase (JGI protein ID: 471060).[58]

Cluster 55-geranylgeranyl pyrophosphate (primary metabolism):

Cluster 55 only encodes a geranylgeranyl pyrophosphate synthase (GGPPS) (JGI protein ID: 182043) which shares 68% identify to Nod ggs1 from *Hypoxylon pulicicidum.*[60] (Figure 4E) Being the only copy of GGPPS in the genome, this protein is likely a house-keeping enzyme which produces GGPP for protein prenylation and ubiquinone biosynthesis. Two genes, predicted to encode cell division control protein and peroxisomal membrane protein are colocalized with GGPPS. To our knowledge, these two proteins are not biosynthetically related and likely to be conserved because of horizontal gene transfer.

3.2.4 Additional clusters with proposed metabolites (Figure 5)

Cluster 44-harzianopyridone:

Cluster 44 is highly homologous to the reported *har* BGC from *Trichoderma harzianum* UK175 that biosynthesizes harzianopyridone (**39** in Figure 5A).[61] Harzianopyridone is a potent antifungal agent inhibiting mitochondrial Complex II involved in oxidative phorphorylation.[62] PKS-NRPS (JGI protein ID: 639479) and ER (JGI protein ID: 598988), which are homologous to HarA and HarE, respectively, are proposed to synthesize tetramic acid **40**, which can undergo P450 (JGI protein ID: 500825) catalyzed ring expansion and dephenylation to form the 2-pyridone **41**. Subsequent modifications by P450 (JGI protein ID: 639482) and MT (JGI protein ID: 619766) that are conserved between the two BGCs, can convert **41** to **42**. Finally, the FMO (JGI protein ID: 619763) and MT (JGI protein ID: 619763) catalyze iterative aromatic hydroxylation and *O*-methylation to install the two methoxy groups to give **39**.

Clusters 59 & 60-peptaibols:

Clusters 59 and 60 encode an 18-module NRPS (JGI protein ID: 549215) and a 14-module NRPS (JGI protein ID: 618517), respectively (Figure 5B). Both NRPSs have a *N*-terminal PKS module (KS-AT-ACP) and a *C*-terminal reductase (R) domain, which are hallmarks of peptaibol synthetases. Peptaibols are antimicrobial peptides that self-assemble into ion channels in cell membrane, which leads to membrane leakage and cell death.[63] Indeed, 549125 and 618517 are homologous to Tex1 and Tex2, respectively, from *T. virens.*[64,65] Tex1 produces an 18-residue peptaibol while Tex2 is responsible for the biosynthesis of 11- and 14-residue peptaibols (an example **43** is shown in Figure 5B). The *N*-terminal PKS module catalyzes the *N*-terminal acetylation of the peptaibols. The last R domain is involved in reduction of the *C*-terminal carboxylate (or a thioester) to an alcohol. One additional feature of peptaibols is the incorporation of the non-canonical amino acids 2-aminoisobutyric acid (Aib, **44**) and isovaline (Iva, **45**). These two unusual amino acids are biosynthesized by a three-enzyme cascade TqaL, TqaF, and TqaM, which were recently characterized from *Penicillium aethiopicum.*[66] Genes encoding these three enzymes (JGI protein IDs: 591073, 507903 and 510569, respectively) are not found in either cluster, but are scattered elsewhere in the ThT22 genome.

3.3. Activation of an unknown BGC from ThT22 by heterologous expression

Combining the four BGCs previously characterized from ThT22 and the bioinformatic dereplication describe above, 25 of the 64 BGCs predicted by AntiSMASH (seven PKSs, nine NRPSs, three PKS-NRPSs, and six terpenes) can be associated, or proposed with high confidence to be associated, with known natural products or primary metabolites (Figure 1A, 1B, and 1D). The remaining majority of predicted BGCs cannot be readily associated with known natural products, either because the biosynthetic pathways have not been characterized, or the BGCs are not homologous to known pathways. Mining these unexplored BGCs should complete inventory of secondary metabolome from ThT22.

We chose to characterize an unknown BGC, cluster 5, by heterologous reconstitution in the model host *A. nidulans* A1145 ΔEMΔST,[27] which has been routinely used for mining and probing fungal natural product BGCs.[20] This BGC encodes five genes: a HRPKS EujE (JGI protein ID: 241969) with a *C*-terminal reductase (R) domain, *trans*-acting enoylreductase (ER) EujC (JGI protein ID: 789593), SDR EujB (JGI protein ID: 521911), P450 EujD (JGI protein ID: 489595), and FMO EujA (JGI protein ID: 489590) (Figure 6A, Supporting Information Table S2). This cluster shares similarity to the betaenone BGC which also contains a HRPKS Bet1 with a *C*-terminal R domain (45% identical to EujE), a *trans*-acting ER Bet3 (50% identical to EujC), a SDR Bet4 (44% identical to EujB), a P450 Bet2 (34% identical to EujD), and a FMO of unknown function (41% identical to EujA).[67] EujE, EujC, and EujB are homologous to the Bet homologs, suggesting that the product of these three enzymes is likely a decalin polyketide with the terminal carboxylate reduced to an alcohol. However, the P450 EujD is only distantly related with Bet2 which is essential for modification of the decalin ring. Therefore, we propose cluster 5 likely encodes a different product than the *bet* BGC. When EujA-EujE were expressed in *A. nidulans*, the transformant produced a compound (**46** in Figure 6B) with high titer (~250 mg/L culture). Structural characterization by NMR and HRMS confirmed compound **46** as eujavanicol A (Supporting Information Figure S2-S7), which was isolated from *Eupenicillium javanicum* IFM 54704 and *T. harzianum* F031, but not from ThT22 prior to this study.[68,69]

We then expressed different combinations of genes in *A. nidulans* to elucidate the function of each enzyme (Figure 6B, 6C). When only HRPKS EujE and *trans*-ER EujC were co-expressed, we observed a new metabolite with molecular mass of 290, which corresponds to decalin bearing compound **47** with a terminal aldehyde. We also observed a cometabolite with a molecular mass of 292, which is likely the alcohol **48** after the aldehyde group in **47** is reduced by endogenous enzymes. This reduction is complete when SDR EujB is coexpressed, suggesting EujB is the dedicate reductase. Co-expression of P450 EujD with EujB, EujC and EujE led to production of eujavanicol A **46**, demonstrating that EujD can catalyze two hydroxylation steps at C5 and C6 to convert **48** to **46**. Coexpression of FMO EujA did not lead to further modification of eujavanicol A. Instead, the presence of this enzyme increased the titer of eujavanicol A in the heterologous host.

3.4. Transcriptomic and metabolomic analysis of ThT22 cultured on different media

While heterologous reconstitution is a powerful approach for characterizing unknown BGCs, a more direct approach with the native host ThT22 is to simultaneously activate multiple silent BGCs by changing culturing conditions.[19] Conditions that can be varied include media components, pH and salinity, culturing vessel, temperature, aeration and light conditions, small molecule additives, and coculturing with another organism. This approach, termed "one strain many compounds" (OSMAC), has been applied to many bacteria and fungi species to elicit production of new and bioactive natural products that are not observed under a single culturing condition.[70] Except for homodimericin A, all other known ThT22 metabolites were isolated by directly culturing the fungus on potato dextrose (PD) media.[12,16] Since overproduction of a metabolite should be accompanied by upregulation of its BGC on a certain medium, the association between BGCs and their corresponding metabolites may be established via transcription analysis of BGCs under OSMAC conditions. Moreover, since genes responsible for the biosynthesis of a metabolite should be coregulated, the relative transcription levels of genes near a core gene (PKS, NRPS, etc) can also be used to define the boundary of a BGC.

We cultured ThT22 on six different media and performed untargeted transcriptomics and metabolic analysis after 7 days. The media used are CD, CGN, MMK2, PDA, V8, and the SSC medium that contains starch, soybean flour, and cottonseed flour as the main nutrient sources (see Materials and Methods). The transcription levels (expressed as reads per kilobase per million mapped reads (RPKM)) of BGCs when ThT22 is grown on the minimal CD medium were used as the reference level for comparison. As shown in Figure 7, while the transcription levels of biosynthetic core genes on CD, V8, and MMK2 are similarly low, most core genes that encode PKSs, NRPSs or terpene cyclases were upregulated on CGN, PDA, and SSC. Notably, SSC exhibits a distinct and complementary core gene transcriptome profile to that of CGN and PDA, suggesting that SSC might be able to activate BGCs that are normally silent on PDA and other media. Indeed, eight BGCs associated with known metabolites were specifically upregulated on SSC media (Figure 8A). Three known metabolites, trichoxide, tricholignan A, and dichlorodiaporthin, can only be detected in extracts of ThT22 grown on SSC (Figure 8B). In addition, six compounds previously not associated with ThT22, including trichoxide, dichlorodiaporthin, destruxin, fumicicolin A, 18-residue peptaibols, and 14-residue peptaibols, were produced from at least one medium (Figure 8B).

Our analysis also revealed a complex relationship between transcription and metabolite levels of known BGCs. In some cases, such as dichlorodiaporthin and tricholignan A, upregulation of a BGC when grown on certain medium is indeed accompanied by detection of the corresponding metabolite (Figure 8, Supporting Information Figure S8). However, this is not the case for most dereplicated BGCs. For example, harzianic acid, t22 azaphilone, pachybasin, destruxin, and fumicicolin A were detected on multiple media despite that their BGCs were only upregulated on a single medium (Figure 8, Figure 9, Supporting Information Figure S9). Conversely, BGCs of eujavanicol A, ferricrocin, trihazone, trichobrasilenol, trichoacorenol, and tricinoloniol acids were all upregulated on at least one medium but showed no accumulation of their corresponding products on any medium (Figure 7, Figure 8, Supporting Information Figure S10). In addition, we observed that genes outside the predicted BGCs can be co-

upregulated with biosynthetic genes. As shown in Figure 9A, four genes near the harzianic acid BGC (JGI protein IDs: 573702 (transcription factor), 476858 (aldehyde dehydrogenase), 207786 (transcription factor), and 548020 (SDR)) are co-upregulated with genes within the BGC on PDA medium. These four proteins are neither conserved nor required for biosynthesis of harzianic acid. In an interesting case shown in Figure 9B, all 10 conserved genes in the t22 azaphilone BGC are co-upregulated on SSC medium while only four of them (JGI protein IDs: 621517, 558993, 293506, 589621) were proposed to be necessary for the biosynthesis.[37] Among the six additional genes, a FMO (JGI protein ID: 532797), a HP (JGI protein ID: 503145), and a DH (JGI protein ID: 599745) may be catalytic but have no proposed function in the pathway. We observed an additional compound from the SSC extract that has very close retention time and same molecular weight as t22 azaphilone (Figure 9B). None of the other media extracts contained this compound. Therefore, it is possible that this compound may be further modified from t22 azaphilone by the functions of these coregulated genes in the BGC.

4. Discussion

Our work here offers a comprehensive view of the biosynthetic inventory of the biocontrol fungus ThT22. ThT22 encodes at least 64 natural products based on BGC prediction, while only seven have been previously described through isolation or genome mining (Figure 1A and 1B). Our bioinformatics dereplication and heterologous reconstitution added potentially up to 22 natural products to the ThT22 metabolite collection (Figure 1D, Table 1). Many of these natural products have agriculturally relevant functions and may collectively play important roles in plant-ThT22 symbiosis. For example, compounds including peptaibols[6] trichoxide,[36] t22 azaphilone,[16] destruxin,[44] harzianic acid,[12] harzianopyridone,[62] and sordarin[59] can form an antifungal and insecticidal arsenal to fight against plant pathogens. The peptaibols in particular are detected as major metabolites on all media we tested (Supporting Figure S9C), suggesting that these molecules may be produced constitutively and act (at least partially) as first line of defense against phytopathogens.[6] Another group of compounds include the siderophores ferricrocin,

tricholignan A, and the unidentified product of cluster 35, can facilitate the acquisition and transport of iron.[18,71]

The remaining 38 unassigned BGCs from ThT22 produce unknown products, and represent a source for genome mining. For example, none of the five lipopeptide BGCs, which contain NRPSs with a characteristic *N*-terminal C domain, has been characterized or has homologous BGCs (Table 1). A recent study has demonstrated antifungal activity of bacterial lipopeptide keanumycins against plant pathogen *Botrytis cinerea.*[72] These ThT22 lipopeptide BGCs may be a promising source for new antifungal agents. In addition, the BGCs we discussed so far all have a core biosynthetic gene that has been used as the hallmark for the genome mining of natural products. The recent application of mining "unknown-unknown" BGC (core gene unpredictable by bioinformatics and compound structure unknown) demonstrated that clusters featuring an atypical core gene can produce compounds with new structures and bioactivity profiles.[73] It is likely that the true biosynthetic space of ThT22 is much larger than what we defined here due to these biosynthetic "dark matters".

The exploration of this large unknown biosynthetic space using genome mining is challenging. As demonstrated by our reconstitution of cluster 5 to make eujavanicol A, rediscovery of the known natural products is commonly encountered. The OSMAC approach, on the other hand, is a simple yet effective way to activate multiple silent BGCs simultaneously and lead to discovery of known and new natural products. In a recent example, *T. harzianum* XS-20090075 was cultured on a rice based medium as well as Czapek's medium to activate production of natural products, including the novel 2-bromo-4-chloroquinoline-3-carboxylate.[74] Similar approach was also applied to *T. harzianum* M10 by varying five different media together with altering light intensity and shaking conditions, which led to the discovery of a new compound 5-hydroxy-2,3-dimethyl-7-methoxychromone.[75] In addition, the ThT22 metabolite homodimericin A was discovered via OSMAC as its production is elicited by a bacterial metabolite bafilomycin C1.[17] Adding to these successful examples, we showed that many compounds previously not observed from ThT22 were elicited by different media, especially SSC (Figure 8). Most core genes from

unknown BGCs are transcriptionally upregulated on this medium (Figure 7). We cannot yet, however, pinpoint the BGC of a compound elicited under a specific condition using transcription analysis. Our results showed that upregulation of a BGC is not always accompanied by accumulation of its metabolite and vice versa (Figure 8, Figure 9). This may be explained by the fact that posttranscription factors such as translation rates and protein stability also impact the secondary metabolite production.[76] More research efforts are needed to reveal the link between the transcriptome, proteome, and metabolome of ThT22 which in return will facilitate OSMAC for natural product discovery.

ThT22 has been widely used as a biocontrol agent and a biofertilizer for over two decades, yet the role of its secondary metabolome in the plant-fungi interaction remains poorly understood. Our study expanded the number of known metabolites of ThT22 which can now be systematically evaluated for their agricultural applications. Our results serve as a starting point for exploring the remaining unassigned BGCs. With the genomes of more than 80 *Trichoderma* species available in public databases (NCBI and JGI), our approach can serve as a model for accessing the biosynthetic potential of this family of agriculturally important fungi, which in turn can facilitate discovery of novel natural products with agricultural significance.

Supporting Information

Additional tables and figures such as DNA primers used in the study, NMR spectrums of eujavanicol A, and additional transcription and metabolic profiles of BGCs with confirmed/proposed products are included in Supporting Information (PDF).

Author information

Corresponding Authors

Yi Tang - Department of Chemical and Biomolecular Engineering, University of California, Los Angeles, California 90095, United States; Department of Chemistry and Biochemistry, University of California, Los Angeles, California 90095, United States; Email: yitang@ucla.edu

Zuodong Sun - Department of Chemical and Biomolecular Engineering, University of California, Los Angeles, California 90095, United States; Email: zsun12@ucla.edu

Authors

Wenyu Han - Department of Chemistry and Biochemistry, University of California, Los Angeles, California 90095, United States

Zhongshou Wu - Department of Molecular Cell and Developmental Biology, University of California, Los Angeles, CA 90095, United States

Zhenhui Zhong - Department of Molecular Cell and Developmental Biology, University of California, Los Angeles, CA 90095, United States

Jason Williams - Department of Chemistry and Biochemistry, University of California, Los Angeles, California 90095, United States

Steven E. Jacobsen - Department of Molecular Cell and Developmental Biology, University of California, Los Angeles, California 90095, United States; Howard Hughes Medical Institute, University of California, Los Angeles, California 90095, United States; Eli & Edythe Broad Center of Regenerative

Medicine & Stem Cell Research, University of California, Los Angeles, California 90095, United States; Department of Biological Chemistry, Los Angeles, California 90095, United States; Email: jacobsen@ucla.edu

Notes

The authors declare no competing financial interest.

Acknowledgement

This study is supported by NIFA (2021-67013-34259). We thank Suhua Feng, Mahnaz Akhavan, and the Broad Stem Cell Research Center Biosequencing core for sequencing. S.E.J. is an investigator of the Howard Hughes Medical Institute.

References:

(1) Raza, A.; Razzaq, A.; Mehmood, S. S.; Zou, X.; Zhang, X.; Lv, Y.; Xu, J. Impact of Climate Change on Crops Adaptation and Strategies to Tackle Its Outcome: A Review. *Plants* **2019**, *8*, 34.

(2) Savary, S.; Willocquet, L.; Pethybridge, S. J.; Esker, P.; McRoberts, N.; Nelson, A. The Global Burden of Pathogens and Pests on Major Food Crops. *Nat. Ecol. Evol.* **2019**, *3*, 430–439.

(3) Lorito, M.; Woo, S. L.; Harman, G. E.; Monte, E. Translational Research on Trichoderma: From'omics to the Field. *Annu. Rev. Phytopathol.* **2010**, *48*, 395–417.

(4) Chaverri, P.; Branco-Rocha, F.; Jaklitsch, W.; Gazis, R.; Degenkolb, T.; Samuels, G. J. Systematics of the Trichoderma Harzianum Species Complex and the Re-Identification of Commercial Biocontrol Strains. *Mycologia* **2015**, *107*, 558–590.

(5) Harman, G. E. Myths and Dogmas of Biocontrol Changes in Perceptions Derived from Research on Trichoderma Harzinum T-22. *Plant Dis.* **2000**, *84*, 377–393.

(6) Schirmböck, M.; Lorito, M.; Wang, Y. L.; Hayes, C. K.; Arisan-Atac, I.; Scala, F.; Harman, G. E.; Kubicek, C. P. Parallel Formation and Synergism of Hydrolytic Enzymes and Peptaibol Antibiotics, Molecular Mechanisms Involved in the Antagonistic Action of Trichoderma Harzianum against Phytopathogenic Fungi. *Appl. Environ. Microbiol.* **1994**, *60*, 4364–4370.

(7) Altomare, C.; Norvell, W. A.; Björkman, T.; Harman, G. E. Solubilization of Phosphates and Micronutrients by the Plant-Growth-Promoting and Biocontrol Fungus Trichoderma Harzianum Rifai 1295-22. *Appl. Environ. Microbiol.* **1999**, *65*, 2926–2933.

(8) Yedidia, I.; Benhamou, N.; Chet, I. Induction of Defense Responses in Cucumber Plants (Cucumis Sativus L.) by the Biocontrol AgentTrichoderma Harzianum. *Appl. Environ. Microbiol.* **1999**, *65*, 1061–1070.

(9) Vinale, F.; Sivasithamparam, K.; Ghisalberti, E. L.; Marra, R.; Barbetti, M. J.; Li, H.; Woo, S. L.; Lorito, M. A Novel Role for Trichoderma Secondary Metabolites in the Interactions with Plants.

Physiol. Mol. Plant Pathol. **2008**, *72*, 80–86.

(10) Contreras-Cornejo, H. A.; Macías-Rodríguez, L.; Del-Val, E.; Larsen, J. Ecological Functions of Trichoderma Spp. and Their Secondary Metabolites in the Rhizosphere: Interactions with Plants. *FEMS Microbiol. Ecol.* **2016**, *92*, fiw036.

(11) Cai, F.; Yu, G.; Wang, P.; Wei, Z.; Fu, L.; Shen, Q.; Chen, W. Harzianolide, a Novel Plant Growth Regulator and Systemic Resistance Elicitor from Trichoderma Harzianum. *Plant Physiol. Biochem.* **2013**, *73*, 106–113.

(12) Xie, L.; Zang, X.; Cheng, W.; Zhang, Z.; Zhou, J.; Chen, M.; Tang, Y. Harzianic Acid from Trichoderma Afroharzianum Is a Natural Product Inhibitor of Acetohydroxyacid Synthase. *J. Am. Chem. Soc.* **2021**, *143*, 9575–9584.

(13) Yan, Y.; Liu, Q.; Zang, X.; Yuan, S.; Bat-Erdene, U.; Nguyen, C.; Gan, J.; Zhou, J.; Jacobsen, S. E.; Tang, Y. Resistance-Gene-Directed Discovery of a Natural-Product Herbicide with a New Mode of Action. *Nature* **2018**, *559*, 415–418.

(14) Zhang, J.-L.; Tang, W.-L.; Huang, Q.-R.; Li, Y.-Z.; Wei, M.-L.; Jiang, L.-L.; Liu, C.; Yu, X.; Zhu, H.-W.; Chen, G.-Z.; Zhang, X.-X. Trichoderma: A Treasure House of Structurally Diverse Secondary Metabolites With Medicinal Importance. *Front. Microbiol.* **2021**, *12*, 723828.

(15) United States Environmental Protection Agency. *Biopesticide Active Ingredients*. https://www.epa.gov/ingredients-used-pesticide-products/biopesticide-active-ingredients (most recent access: April 17, 2023).

(16) Vinale, F.; Marra, R.; Scala, F.; Ghisalberti, E. L.; Lorito, M.; Sivasithamparam, K. Major Secondary Metabolites Produced by Two Commercial Trichoderma Strains Active against Different Phytopathogens. *Lett. Appl. Microbiol.* **2006**, *43*, 143–148.

(17) Mevers, E.; Saurí, J.; Liu, Y.; Moser, A.; Ramadhar, T. R.; Varlan, M.; Williamson, R. T.; Martin, G. E.; Clardy, J. Homodimericin A: A Complex Hexacyclic Fungal Metabolite. *J. Am. Chem. Soc.* **2016**, *138*, 12324–12327.

(18) Chen, M.; Liu, Q.; Gao, S.-S.; Young, A. E.; Jacobsen, S. E.; Tang, Y. Genome Mining and Biosynthesis of a Polyketide from a Biofertilizer Fungus That Can Facilitate Reductive Iron Assimilation in Plant. *Proc. Natl. Acad. Sci.* **2019**, *116*, 5499–5504.

(19) Rutledge, P. J.; Challis, G. L. Discovery of Microbial Natural Products by Activation of Silent Biosynthetic Gene Clusters. *Nat. Rev. Microbiol.* **2015**, *13*, 509–523.

(20) Chiang, C.-Y.; Ohashi, M.; Tang, Y. Deciphering Chemical Logic of Fungal Natural Product Biosynthesis through Heterologous Expression and Genome Mining. *Nat. Prod. Rep.* **2023**, *40*, 89–127.

(21) Shenouda, M. L.; Cox, R. J. Molecular Methods Unravel the Biosynthetic Potential of Trichoderma Species. *RSC Adv.* **2021**, *11*, 3622–3635.

(22) Zhu, Y. G.; Wang, J. F.; Mou, P. Y.; Yan, Y.; Chen, M. B.; Tang, Y. Genome Mining of Cryptic Tetronate Natural Products from a PKS-NRPS Encoding Gene Cluster in Trichoderma Harzianum t-22. *Org. Biomol. Chem.* **2021**, *19*, 1985–1990.

(23) Nordberg, H.; Cantor, M.; Dusheyko, S.; Hua, S.; Poliakov, A.; Shabalov, I.; Smirnova, T.; Grigoriev, I. V; Dubchak, I. The Genome Portal of the Department of Energy Joint Genome Institute: 2014 Updates. *Nucleic Acids Res.* **2014**, *42*, D26–D31.

(24) Blin, K.; Shaw, S.; Steinke, K.; Villebro, R.; Ziemert, N.; Lee, S. Y.; Medema, M. H.; Weber, T. AntiSMASH 5.0: Updates to the Secondary Metabolite Genome Mining Pipeline. *Nucleic Acids Res.* **2019**, gkz310.

(25) *2ndFind*. https://biosyn.nih.go.jp/2ndfind/.

(26) Sun, Z.; Jamieson, C. S.; Ohashi, M.; Houk, K. N.; Tang, Y. Discovery and Characterization of a Terpene Biosynthetic Pathway Featuring a Norbornene-Forming Diels-Alderase. *Nat. Commun.* **2022**, *13*, 2568.

(27) Liu, N.; Hung, Y.-S.; Gao, S.-S.; Hang, L.; Zou, Y.; Chooi, Y.-H.; Tang, Y. Identification and Heterologous Production of a Benzoyl-Primed Tricarboxylic Acid Polyketide Intermediate from

the Zaragozic Acid A Biosynthetic Pathway. *Org. Lett.* **2017**, *19*, 3560–3563.

(28) Langmead, B.; Salzberg, S. L. Fast Gapped-Read Alignment with Bowtie 2. *Nat. Methods* **2012**, *9*, 357–359.

(29) Li, B.; Dewey, C. N. RSEM: Accurate Transcript Quantification from RNA-Seq Data with or without a Reference Genome. *BMC Bioinformatics* **2011**, *12*, 323.

(30) Kolde, R. Pheatmap: Pretty Heatmaps. *R Packag. version* **2012**, *1*, 726.

(31) Robey, M. T.; Caesar, L. K.; Drott, M. T.; Keller, N. P.; Kelleher, N. L. An Interpreted Atlas of Biosynthetic Gene Clusters from 1,000 Fungal Genomes. *Proc. Natl. Acad. Sci.* **2021**, *118*, e2020230118.

(32) Liu, M.; Ohashi, M.; Hung, Y.-S.; Scherlach, K.; Watanabe, K.; Hertweck, C.; Tang, Y. AoiQ Catalyzes Geminal Dichlorination of 1,3-Diketone Natural Products. *J. Am. Chem. Soc.* **2021**, *143*, 7267–7271.

(33) Hang, L.; Tang, M.; Harvey, C. J. B.; Page, C. G.; Li, J.; Hung, Y.; Liu, N.; Hillenmeyer, M. E.; Tang, Y. Reversible Product Release and Recapture by a Fungal Polyketide Synthase Using a Carnitine Acyltransferase Domain. *Angew. Chemie Int. Ed.* **2017**, *129*, 9684–9688.

(34) Zeng, G.; Zhang, P.; Zhang, Q.; Zhao, H.; Li, Z.; Zhang, X.; Wang, C.; Yin, W.-B.; Fang, W. Duplication of a Pks Gene Cluster and Subsequent Functional Diversification Facilitate Environmental Adaptation in Metarhizium Species. *PLOS Genet.* **2018**, *14*, e1007472.

(35) Frandsen, R. J. N.; Schütt, C.; Lund, B. W.; Staerk, D.; Nielsen, J.; Olsson, S.; Giese, H. Two Novel Classes of Enzymes Are Required for the Biosynthesis of Aurofusarin in Fusarium Graminearum. *J. Biol. Chem.* **2011**, *286*, 10419–10428.

(36) Liu, L.; Tang, M.-C.; Tang, Y. Fungal Highly Reducing Polyketide Synthases Biosynthesize Salicylaldehydes That Are Precursors to Epoxycyclohexenol Natural Products. *J. Am. Chem. Soc.* **2019**, *141*, 19538–19541.

(37) Pang, G.; Sun, T.; Yu, Z.; Yuan, T.; Liu, W.; Zhu, H.; Gao, Q.; Yang, D.; Kubicek, C. P.; Zhang,

J. Azaphilones Biosynthesis Complements the Defence Mechanism of Trichoderma Guizhouense against Oxidative Stress. *Environ. Microbiol.* **2020**, *22*, 4808–4824.

(38) Zabala, A. O.; Xu, W.; Chooi, Y. H.; Tang, Y. Characterization of a Silent Azaphilone Gene Cluster from Aspergillus Niger ATCC 1015 Reveals a Hydroxylation-Mediated Pyran-Ring Formation. *Chem. Biol.* **2012**, *19*, 1049–1059.

(39) Matsuda, Y.; Gotfredsen, C. H.; Larsen, T. O. Genetic Characterization of Neosartorin Biosynthesis Provides Insight into Heterodimeric Natural Product Generation. *Org. Lett.* **2018**, *20*, 7197–7200.

(40) Kim, S.-J.; Kim, M.-C.; Lee, B.-J.; Park, D.-H.; Hong, S.-H.; Um, J.-Y. Anti-Inflammatory Activity of Chrysophanol through the Suppression of NF-KappaB/Caspase-1 Activation in Vitro and in Vivo. *Molecules* **2010**, *15*, 6436–6451.

(41) Lin, Y.-R.; Peng, K.-C.; Chan, M.-H.; Peng, H.-L.; Liu, S.-Y. Effect of Pachybasin on General Toxicity and Developmental Toxicity in Vivo. *J. Agric. Food Chem.* **2017**, *65*, 10489–10494.

(42) Delgadillo, D., Burch, J., Kim, L. J., de Moraes, L., Niwa, K., Williams, J., Tang, M., Lavallo, V., Chhetri, B., Jones, C., Hernandez Rodriguez, I., Signore, J., Marquez, L., Bhanushali, R., Greene, M., Woo, S., Kubanek, J., Quave, C., Tang, Y.; Nelson, H. High-Throughput Identification of Crystalline Natural Products from Crude Extracts Enabled by Microarray Technology and MicroED. *ChemRxiv* **2023**, No. This content is a preprint and has not been peer-reviewed.

(43) Wang, B.; Kang, Q.; Lu, Y.; Bai, L.; Wang, C. Unveiling the Biosynthetic Puzzle of Destruxins in Metarhizium Species. *Proc. Natl. Acad. Sci.* **2012**, *109*, 1287–1292.

(44) Liu, B.-L.; Tzeng, Y.-M. Development and Applications of Destruxins: A Review. *Biotechnol. Adv.* **2012**, *30*, 1242–1254.

(45) Wang, Y.; Hu, P. J.; Pan, Y. Y.; Zhu, Y. X.; Liu, X. Z.; Che, Y. S.; Liu, G. Identification and Characterization of the Verticillin Biosynthetic Gene Cluster in Clonostachys Rogersoniana.

Fungal Genet. Biol. **2017**, *103*, 25–33.

(46) Son, B. W.; Jensen, P. R.; Kauffman, C. A.; Fenical, W. New Cytotoxic Epidithiodioxopiperazines Related to Verticillin A From A Marine Isolate of the Fungus Penicillium. *Nat. Prod. Lett.* **1999**, *13*, 213–222.

(47) Scharf, D. H.; Heinekamp, T.; Remme, N.; Hortschansky, P.; Brakhage, A. A.; Hertweck, C. Biosynthesis and Function of Gliotoxin in Aspergillus Fumigatus. *Appl. Microbiol. Biotechnol.* **2012**, *93*, 467–472.

(48) Mazzaferro, L. S.; Hüttel, W.; Fries, A.; Müller, M. Cytochrome P450-Catalyzed Regio- and Stereoselective Phenol Coupling of Fungal Natural Products. *J. Am. Chem. Soc.* **2015**, *137*, 12289–12295.

(49) Tobiasen, C.; Aahman, J.; Ravnholt, K. S.; Bjerrum, M. J.; Grell, M. N.; Giese, H. Nonribosomal Peptide Synthetase (NPS) Genes in Fusarium Graminearum, F. Culmorum and F. Pseudograminearium and Identification of NPS2 as the Producer of Ferricrocin. *Curr. Genet.* **2007**, *51*, 43–58.

(50) Hai, Y.; Huang, A. M.; Tang, Y. Structure-Guided Function Discovery of an NRPS-like Glycine Betaine Reductase for Choline Biosynthesis in Fungi. *Proc. Natl. Acad. Sci. U. S. A.* **2019**, *116*, 10348–10353.

(51) Won, T. H.; Bok, J. W.; Nadig, N.; Venkatesh, N.; Nickles, G.; Greco, C.; Lim, F. Y.; González, J. B.; Turgeon, B. G.; Keller, N. P.; Schroeder, F. C. Copper Starvation Induces Antimicrobial Isocyanide Integrated into Two Distinct Biosynthetic Pathways in Fungi. *Nat. Commun.* **2022**, *13*, 4828.

(52) Schrettl, M.; Bignell, E.; Kragl, C.; Sabiha, Y.; Loss, O.; Eisendle, M.; Wallner, A.; Arst Jr., H. N.; Haynes, K.; Haas, H. Distinct Roles for Intra- and Extracellular Siderophores during Aspergillus Fumigatus Infection. *PLOS Pathog.* **2007**, *3*, e128.

(53) Casqueiro, J.; Gutiérrez, S.; Bañuelos, O.; Fierro, F.; Velasco, J.; Martín, J. F. Characterization of

the Lys2 Gene of Penicillium Chrysogenum Encoding α-Aminoadipic Acid Reductase. *Mol. Gen. Genet.* **1998**, *259*, 549–556.

(54) Murai, K.; Lauterbach, L.; Teramoto, K.; Quan, Z.; Barra, L.; Yamamoto, T.; Nonaka, K.; Shiomi, K.; Nishiyama, M.; Kuzuyama, T.; Dickschat, J. S. An Unusual Skeletal Rearrangement in the Biosynthesis of the Sesquiterpene Trichobrasilenol from Trichoderma. *Angew. Chemie Int. Ed.* **2019**, *58*, 15046–15050.

(55) Wen, Y.-H.; Chen, T.-J.; Jiang, L.-Y.; Li, L.; Guo, M.; Peng, Y.; Chen, J.-J.; Pei, F.; Yang, J.-L.; Wang, R.-S.; Gong, T.; Zhu, P. Unusual (2R,6R)-Bicyclo[3.1.1]Heptane Ring Construction in Fungal α-Trans-Bergamotene Biosynthesis. *iScience* **2022**, *25*, 104030.

(56) Da Silva Ferreira, M. E.; Colombo, A. L.; Paulsen, I.; Ren, Q.; Wortman, J.; Huang, J.; Goldman, M. H. S.; Goldman, G. H. The Ergosterol Biosynthesis Pathway, Transporter Genes, and Azole Resistance in Aspergillus Fumigatus. *Med. Mycol.* **2005**, *43*, S313–S319.

(57) Liu, H.; Pu, Y.-H.; Ren, J.-W.; Li, E.-W.; Guo, L.-X.; Yin, W.-B. Genetic Dereplication Driven Discovery of a Tricinoloniol Acid Biosynthetic Pathway in Trichoderma Hypoxylon. *Org. Biomol. Chem.* **2020**, *18*, 5344–5348.

(58) Kudo, F.; Matsuura, Y.; Hayashi, T.; Fukushima, M.; Eguchi, T. Genome Mining of the Sordarin Biosynthetic Gene Cluster from Sordaria Araneosa Cain ATCC 36386: Characterization of Cycloaraneosene Synthase and GDP-6-Deoxyaltrose Transferase. *J. Antibiot. (Tokyo).* **2016**, *69*, 541–548.

(59) Justice, M. C.; Hsu, M.-J.; Tse, B.; Ku, T.; Balkovec, J.; Schmatz, D.; Nielsen, J. Elongation Factor 2 as a Novel Target for Selective Inhibition of Fungal Protein Synthesis. *J. Biol. Chem.* **1998**, *273*, 3148–3151.

(60) Van de Bittner, K. C.; Nicholson, M. J.; Bustamante, L. Y.; Kessans, S. A.; Ram, A.; van Dolleweerd, C. J.; Scott, B.; Parker, E. J. Heterologous Biosynthesis of Nodulisporic Acid F. *J. Am. Chem. Soc.* **2018**, *140*, 582–585.

(61) Bat-Erdene, U.; Kanayama, D.; Tan, D.; Turner, W. C.; Houk, K. N.; Ohashi, M.; Tang, Y. Iterative Catalysis in the Biosynthesis of Mitochondrial Complex II Inhibitors Harzianopyridone and Atpenin B. *J. Am. Chem. Soc.* **2020**, *142*, 8550–8554.

(62) Miyadera, H.; Shiomi, K.; Ui, H.; Yamaguchi, Y.; Masuma, R.; Tomoda, H.; Miyoshi, H.; Osanai, A.; Kita, K.; Ōmura, S. Atpenins, Potent and Specific Inhibitors of Mitochondrial Complex II (Succinate-Ubiquinone Oxidoreductase). *Proc. Natl. Acad. Sci.* **2003**, *100*, 473–477.

(63) Chugh, J. K.; Wallace, B. A. Peptaibols: Models for Ion Channels. *Biochem. Soc. Trans.* **2001**, *29*, 565–570.

(64) Wiest, A.; Grzegorski, D.; Xu, B.-W.; Goulard, C.; Rebuffat, S.; Ebbole, D. J.; Bodo, B.; Kenerley, C. Identification of Peptaibols from Trichoderma Virens and Cloning of a Peptaibol Synthetase. *J. Biol. Chem.* **2002**, *277*, 20862–20868.

(65) Mukherjee, P. K.; Wiest, A.; Ruiz, N.; Keightley, A.; Moran-Diez, M. E.; McCluskey, K.; Pouchus, Y. F.; Kenerley, C. M. Two Classes of New Peptaibols Are Synthesized by a Single Non-Ribosomal Peptide Synthetase of Trichoderma Virens. *J. Biol. Chem.* **2011**, *286*, 4544–4554.

(66) Bunno, R.; Awakawa, T.; Mori, T.; Abe, I. Aziridine Formation by a FeII/α-Ketoglutarate Dependent Oxygenase and 2-Aminoisobutyrate Biosynthesis in Fungi. *Angew. Chemie Int. Ed.* **2021**, *60*, 15827–15831.

(67) Ugai, T.; Minami, A.; Fujii, R.; Tanaka, M.; Oguri, H.; Gomi, K.; Oikawa, H. Heterologous Expression of Highly Reducing Polyketide Synthase Involved in Betaenone Biosynthesis. *Chem. Commun.* **2015**, *51*, 1878–1881.

(68) Nakadate, S.; Nozawa, K.; Horie, H.; Fujii, Y.; Nagai, M.; Hosoe, T.; Kawai, K.; Yaguchi, T.; Fukushima, K. Eujavanicols A–C, Decalin Derivatives from Eupenicillium Javanicum. *J. Nat. Prod.* **2007**, *70*, 1510–1512.

(69) Jeerapong, C.; Phupong, W.; Bangrak, P.; Intana, W.; Tuchinda, P. Trichoharzianol, a New Antifungal from Trichoderma Harzianum F031. *J. Agric. Food Chem.* **2015**, *63*, 3704–3708.

(70) Bode, H. B.; Bethe, B.; Höfs, R.; Zeeck, A. Big Effects from Small Changes: Possible Ways to Explore Nature's Chemical Diversity. *ChemBioChem* **2002**, *3*, 619–627.

(71) Anja, W.; Michael, B.; Markus, S.; Bettina, S.; Herbert, L.; Hubertus, H. Ferricrocin, a Siderophore Involved in Intra- and Transcellular Iron Distribution in Aspergillus Fumigatus. *Appl. Environ. Microbiol.* **2009**, *75*, 4194–4196.

(72) Götze, S.; Vij, R.; Burow, K.; Thome, N.; Urbat, L.; Schlosser, N.; Pflanze, S.; Müller, R.; Hänsch, V. G.; Schlabach, K.; Fazlikhani, L.; Walther, G.; Dahse, H.-M.; Regestein, L.; Brunke, S.; Hube, B.; Hertweck, C.; Franken, P.; Stallforth, P. Ecological Niche-Inspired Genome Mining Leads to the Discovery of Crop-Protecting Nonribosomal Lipopeptides Featuring a Transient Amino Acid Building Block. *J. Am. Chem. Soc.* **2023**, *145*, 2342–2353.

(73) Yee, D. A.; Niwa, K.; Perlatti, B.; Chen, M.; Li, Y.; Tang, Y. Genome Mining for Unknown–Unknown Natural Products. *Nat. Chem. Biol.* **2023**, *19*, 633–640.

(74) Yu, J.-Y.; Shi, T.; Zhou, Y.; Xu, Y.; Zhao, D.-L.; Wang, C.-Y. Naphthalene Derivatives and Halogenate Quinoline from the Coral-Derived Fungus Trichoderma Harzianum (XS-20090075) through OSMAC Approach. *J. Asian Nat. Prod. Res.* **2021**, *23*, 250–257.

(75) Staropoli, A.; Iacomino, G.; De Cicco, P.; Woo, S. L.; Di Costanzo, L.; Vinale, F. Induced Secondary Metabolites of the Beneficial Fungus Trichoderma Harzianum M10 through OSMAC Approach. *Chem. Biol. Technol. Agric.* **2023**, *10*, 28.

(76) Zapalska-Sozoniuk, M.; Chrobak, L.; Kowalczyk, K.; Kankofer, M. Is It Useful to Use Several "Omics" for Obtaining Valuable Results? *Mol. Biol. Rep.* **2019**, *46*, 3597–3606.

(77) Vinale, F.; Manganiello, G.; Nigro, M.; Mazzei, P.; Piccolo, A.; Pascale, A.; Ruocco, M.; Marra, R.; Lombardi, N.; Lanzuise, S.; Varlese, R.; Cavallo, P.; Lorito, M.; Woo, S. L. A Novel Fungal Metabolite with Beneficial Properties for Agricultural Applications. *Molecules* **2014**, *19*, 9760–9772.

(78) Hwang, L. H.; Mayfield, J. A.; Rine, J.; Sil, A. Histoplasma Requires SID1, a Member of an Iron-

Regulated Siderophore Gene Cluster, for Host Colonization. *PLOS Pathog.* **2008**, *4*, e1000044.

(79) Chooi, Y.-H.; Tang, Y. Adding the Lipo to Lipopeptides: Do More with Less. *Chem. Biol.* **2010**, *17*, 791–793.

Figure captions

Figure 1. Overview of natural products and BGCs from ThT22. (**A**), compounds directly isolated from ThT22. (**B**), compounds discovered from ThT22 by genome mining. (**C**), the distribution of ThT22 BGCs by types of natural products. (**D**), compounds that can be produced by ThT22 based on bioinformatics analysis of the BGCs.

Figure 2. ThT22 BGCs homologous to characterized polyketide biosynthetic pathways and their proposed products. The number shown on top of the ThT22 genes are their JGI protein IDs. (**A**), cluster 1 is homologous to a BGC from *T. virens*. (**B**), cluster 7 is homologous to a BGC of an unidentified fungal pigment from *M. anisopliae*. (**C**), cluster 8 is homologous to the trichoxide BGC. (**D**), cluster 12 is homologous to the t22 azaphilone cluster. (**E**), cluster 18 is homologous to the emodin and chrysophanol BGC. Abbreviations: HRPKS, highly reducing polyketide synthase; SDR, short-chain reductase; DUF, domain of unknown family; TF, transcription factor; NRPKS, non-reducing polyketide synthase; HP, hypothetical protein; FMO, flavin-dependent monooxygenase; DH, dehydratase; KS, ketosynthase; AT, acyltransferase; KR, ketoreductase; ER, ene-reductase; ACP, acyl carrier protein; SAT, starter unit acyltransferase; P450, cytochrome P450; GST, glutathione S-transferase; NTF2, NTF2 family protein; EthD, EthD family protein; MT, methyltransferase.

Figure 3. ThT22 BGCs homologous to characterized nonribosomal peptide biosynthetic pathways and their proposed products. (**A**), cluster 20 is homologous to the destruxin BGC. (**B**), cluster 21 is homologous to the verticillin BGC. (**C**), cluster 24 is homologous to the ferricrocin BGC. (**D**), the core gene of cluster 25 is homologous to the glycine betaine reductase from *A. nidulans*. (**E**), cluster 32 is homologous to the fumicicolin A BGC. (**F**), cluster 35 is homologous to a BGC of triacetylfusarinine C from *A. fumigatus*. (**G**), the core gene of cluster 39 is homologous to the L-2-aminoadipate reductase from

Penicillium chrysogenum. Abbreviations: A, adenylation domain; T, thiolation domain; E, epimerization domain; C, condensation domain; *N*-MT, *N*-methyltransferase domain; 2KG, iron and 2-ketoglutarate dependent enzyme; ICS, isocyanide synthase.

Figure 4. ThT22 terpene BGCs homologous to characterized biosynthetic pathways and their proposed products. (**A**), cluster 46 is homologous to the trichobrasilenol BGC. (**B**), cluster 47 is homologous to the trichoacorenol BGC. (**C**), the core gene of cluster 52 is homologous to the tricinoloniol acid BGC. (**D**), cluster 54 is homologous to the sordarin BGC. (**E**), the core gene of cluster 55 is homologous to a GGPPS from *Hypoxylon pulicicidum.* Abbreviations: TC, terpene cyclase; GGPP, geranylgeranyl pyrophosphate; FPP, farnesyl pyrophosphate; DAase, Diels-Alderase.

Figure 5. Additional ThT22 BGCs homologous to characterized biosynthetic pathways and their proposed products. (**A**), cluster 44 is homologous to the harzianopyridone BGC. (**B**), clusters 59 and 60 are homologous to the peptaibol BGC. A sample 14-residue peptaibol Tv29-14S-I b is used for the illustration. Abbreviations: R, reductase domain; O-MT, O-methyltransferase; NHIO, non-heme iron oxygenase.

Figure 6. Reconstitution of cluster 5 in *A. nidulans*, which led to the biosynthesis of eujavanicol A **46**. (**A**), cluster 5 in ThT22. Numbers on top of the genes are their corresponding JGI protein IDs. (**B**), Metabolic analysis of *A. nidulans* transformed with genes in cluster 5. LC-MS traces are shown as extracted ion chromatogram are shown. (**C**), proposed biosynthesis of eujavanicol A.

Figure 7. Relative transcription level of biosynthetic core genes in ThT22 on different media. Colors scaled based on the RPKM number relative to that obtained from growth on CD medium. Three

820 independent data sets are shown for each medium. CD, MMK2, and V8 are commonly used nutrient-
821 deficient media for fungal culture. CGN and PDA are commonly used nutrient-rich media, and the SSC
822 medium is a homemade nutrient-rich media.
823
824 **Figure 8.** Transcription and metabolite profiles of ThT22 BGCs with confirmed and proposed products.
825 (**A**), transcriptional upregulation of known BGCs on different media. (**B**), detection of known metabolites
826 on different media. Metabolic analysis for clusters 1, 7, and 35 are not applicable since the exact products
827 of these clusters are not yet known. Cluster 25 is not applicable since its product choline is a primary
828 metabolite and should be produced under all conditions. The peptaibols we observed have the same
829 masses as the products of Tex1 and Tex2 from *T. virens*.[64,65] Determination of their actual amino acid
830 sequences requires further studies.
831
832 **Figure 9.** Transcription and metabolite profiles of selected BGCs. (**A**), cluster 42-harzianic acid. Besides
833 harzianic acid, we also observed its isomer isoharzianic acid.[77] (**B**), cluster 12-t22 azaphilone. Top panel,
834 BGC and proposed biosynthetic pathway. Bottom left panel, the transcription profile of the BGC and
835 genes nearby on different media. Three independent transcription profiles are shown for each medium.
836 Colors in the heatmaps are scaled based on the RPKM number relative to that of CD. The black box
837 indicates boundary of the BGC (as predicted by gene conservation within homologous BGCs). Bottom
838 right panel, detection of the metabolite encoded by the BGC via LC-MS. One representative metabolic
839 profile of three independent experiments is shown for each medium. Traces are shown as extracted ion
840 chromatograms.

Table

Table 1. Summary of ThT22 BGCs predicted from antiSMASH.[1]

Cluster number	Scaffold number	Secondary metabolite class	Core gene protein ID	Confirmed (C)/proposed (P)/unknown (U) product	Origin of characterized pathway (core gene identity)	Reference
1	1	PK[3]	605427	**1** and **2** (P)	*Trichoderma virens* (91%)	[33]
2	1	PK	605521	(U)	-	
3	2	PK	136974	(U)		
4	3	PK	616799	(U)		
5	4	PK	241969	eujavanicol A **46** (C)	ThT22 (100%)	this work
6	8	PK	623584	(U)		
7	9	PK	624619	conidial pigment (P)	*Metarhizium anisopliae (76%)*	[34]
8	24	PK	615175	trichoxide **3** (P)	*Trichoderma virens* (85%)	[36]
9	41	PK	588563	(U)		
10	42	PK	619181/556449	tricholignan A (C)	ThT22 (100%)	[18]
11	52	PK	620703	(U)		
12	60	PK	621517/558993	t22 azaphilone **7** (P)	*Trichoderma guizhouense* (92%/96%)	[37]
13	74	PK	462023	(U)		
14	88	PK	463838	(U)		
15	96	PK	641822	dichlorodiaporthin (C)	ThT22 (100%)	[32]
16	129[2]	PK	48863	(U)		
17	138[2]	PK	582152	(U)		
18	271[2]	PK	195120	chrysophanol **13** / pachybasin **10** (P)	*Aspergillus novofumigatus* (71%)	[39]
19	277[2]	PK	616175	(U)		
20	1	NRP[4]	626604	destruxin **14** (P)	*Metarhizium robertsii* (53%)	[43]
21	2[2]	NRP	447208	11′-deoxyverticillin A **17** (P)	*Clonostachys rogersoniana (47%)*	[45]
22	3	NRP	585212	(U)		

Cluster number	Scaffold number	Secondary metabolite class	Core gene protein ID	Confirmed (C)/proposed (P)/unknown (U) product	Origin of characterized pathway (core gene identity)	Reference
23	3	NRP	489354	(U)		
24	3	NRP	211076	ferricrocin **22** (P)	*Fusarium graminearum* (51%)	[49]
25	6	NRP	291737	choline **23** (P)	*Aspergillus nidulans* (66%)	[50]
26	7	NRP	549190	(U)		
27	19	NRP	122438	(U)		
28	19	NRP	494647	(U)		
29	30	NRP	576782	(U)		
30	31	NRP	617296	(U)		
31	32	NRP	588060	(U)		
32	48	NRP	531123	fumicicolin A **25** (P)	*Aspergillus fumigatus* (71%)	[51]
33	49[2]	NRP	619995	(U)		
34	60	NRP	621604	(U)		
35	76	NRP	323124	fusarinine-like siderophore **28** (P)	*Aspergillus fumigatus* (42%)	[78]
36	88	NRP	507298	(U)		
37	137	NRP	468785	(U)		
38	139[2]	NRP	609109	(U)		
39	211[2]	NRP	544585	L-2-aminoadipate-δ-semialdehyde (P)	*Penicillium chrysogenum (51%)*	[53]
40	270[2]	NRP	194945	(U)		
41	1	PK-NRP hybrid	605592	(U)		
42	3	PK-NRP hybrid	476860	harzianic acid (C)	ThT22 (100%)	[12]
43	36	PK-NRP hybrid	618089	trihazone (C)	ThT22 (100%)	[22]
44	46	PK-NRP hybrid	639479	harzianopyridone **39** (P)	*Trichoderma harzianum* ATCC 64870 (99%)	[61]
45	61	PK-NRP hybrid	640280	(U)		
46	3	Terpene	210618	trichobrasilenol **29** (P)	*Trichoderma atroviride* (73%)	[54]
47	6	Terpene	291000	trichoacorenol **30** (P)	*Nectria sp.* (74%)	[55]
48	10	Terpene	491870	(U)		
49	28	Terpene	554103	(U)		
50	45	Terpene	619629	(U)		

Cluster number	Scaffold number	Secondary metabolite class	Core gene protein ID	Confirmed (C)/proposed (P)/unknown (U) product	Origin of characterized pathway (core gene identity)	Reference
51	50	Terpene	578267	squalene (P)	*Aspergillus fumigatus* (57%)	[56]
52	69[2]	Terpene	461327	tricinoloniol acid **31** (P)	*Trichoderma hypoxylon* (81%)	[57]
53	83	Terpene	340419	(U)		
54	171	Terpene	593170	sordarin **34** (P)	*Sordaria araneosa* (72%)	[26]
55	256	Terpene	182043	GGPP (P)	*Hypoxylon pulicicidum (68%)*	[60]
56	294	Terpene	475865	(U)		
57	4	RiPP	618844	(U)		
58	3	Lipopeptide[5]	626740	(U)		
59	7	NRP	549215	18-residue peptaibol (P)	*Trichoderma virens* (81%)	[64]
60	39	NRP	618517	14-residue peptaibol (P)	*Trichoderma virens* (80%)	[65]
61	103	Lipopeptide	606133	(U)		
62	106	Lipopeptide	581052	(U)		
63	106	Lipopeptide	606361	(U)		
64	125	Lipopeptide	565773	(U)		

[1] Total number of BGCs, 64; number of BGCs with confirmed metabolites (C), 5; number of BGCs with proposed metabolites (P), 21; number of BGCs with unknown metabolites (U), 38. [2] These clusters are on the edge of a scaffold. [3] PK, polyketide. [4] NRP, non-ribosomal peptide. [5] These clusters all contain a NRPS with a N-terminal condensation (C) domain, which is characteristic of lipopeptide BGCs.[79]

Figure 1

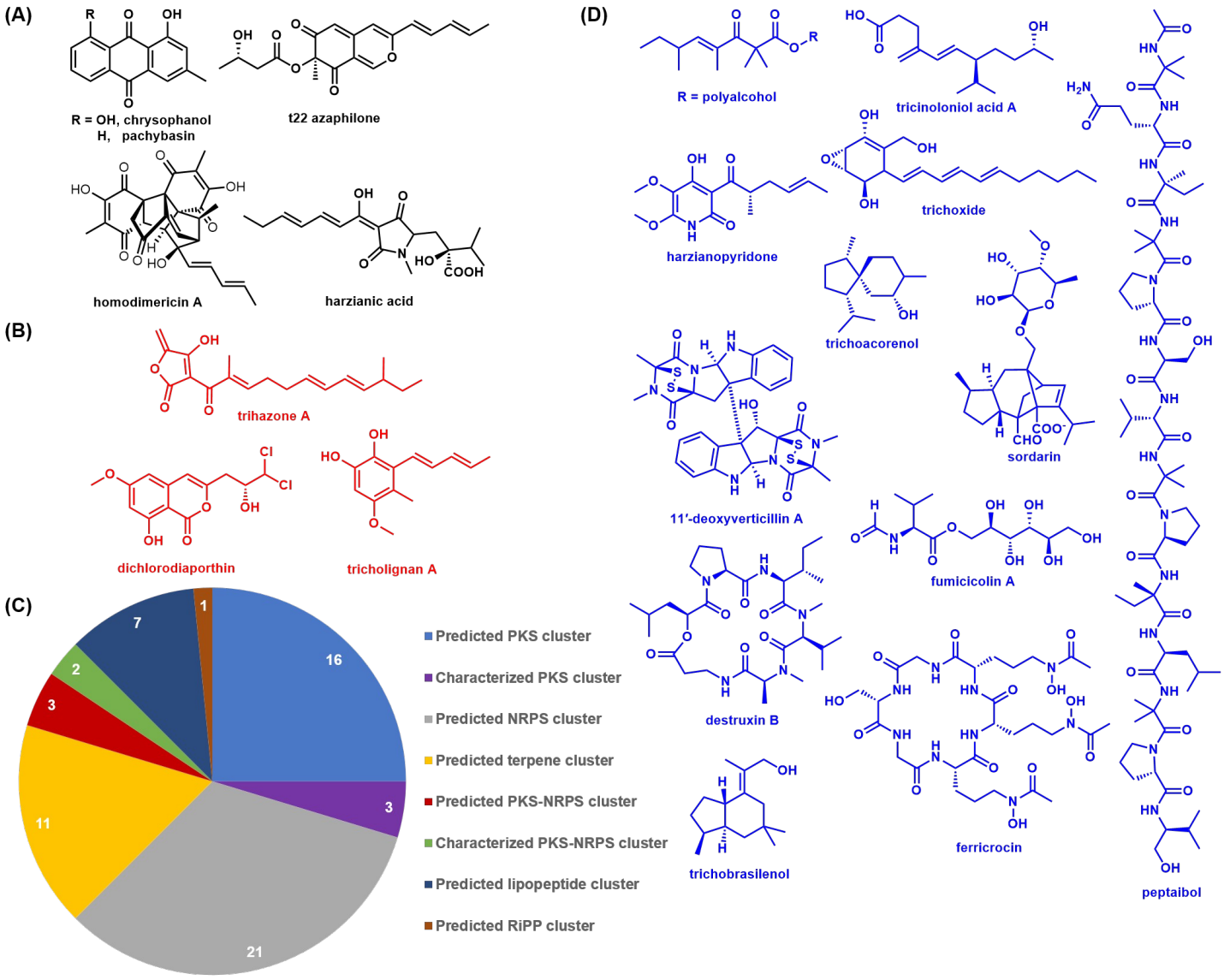
(A)
R = OH, chrysophanol
H, pachybasin
t22 azaphilone
homodimericin A
harzianic acid
(B)
trihazone A
dichlorodiaporthin
tricholignan A
(C)
16
3
21
11
3
2
7
1
Predicted PKS cluster
Characterized PKS cluster
Predicted NRPS cluster
Predicted terpene cluster
Predicted PKS-NRPS cluster
Characterized PKS-NRPS cluster
Predicted lipopeptide cluster
Predicted RiPP cluster
(D)
R = polyalcohol
tricinoloniol acid A
trichoxide
harzianopyridone
trichoacorenol
sordarin
11′-deoxyverticillin A
fumicicolin A
destruxin B
ferricrocin
trichobrasilenol
peptaibol

Figure 2

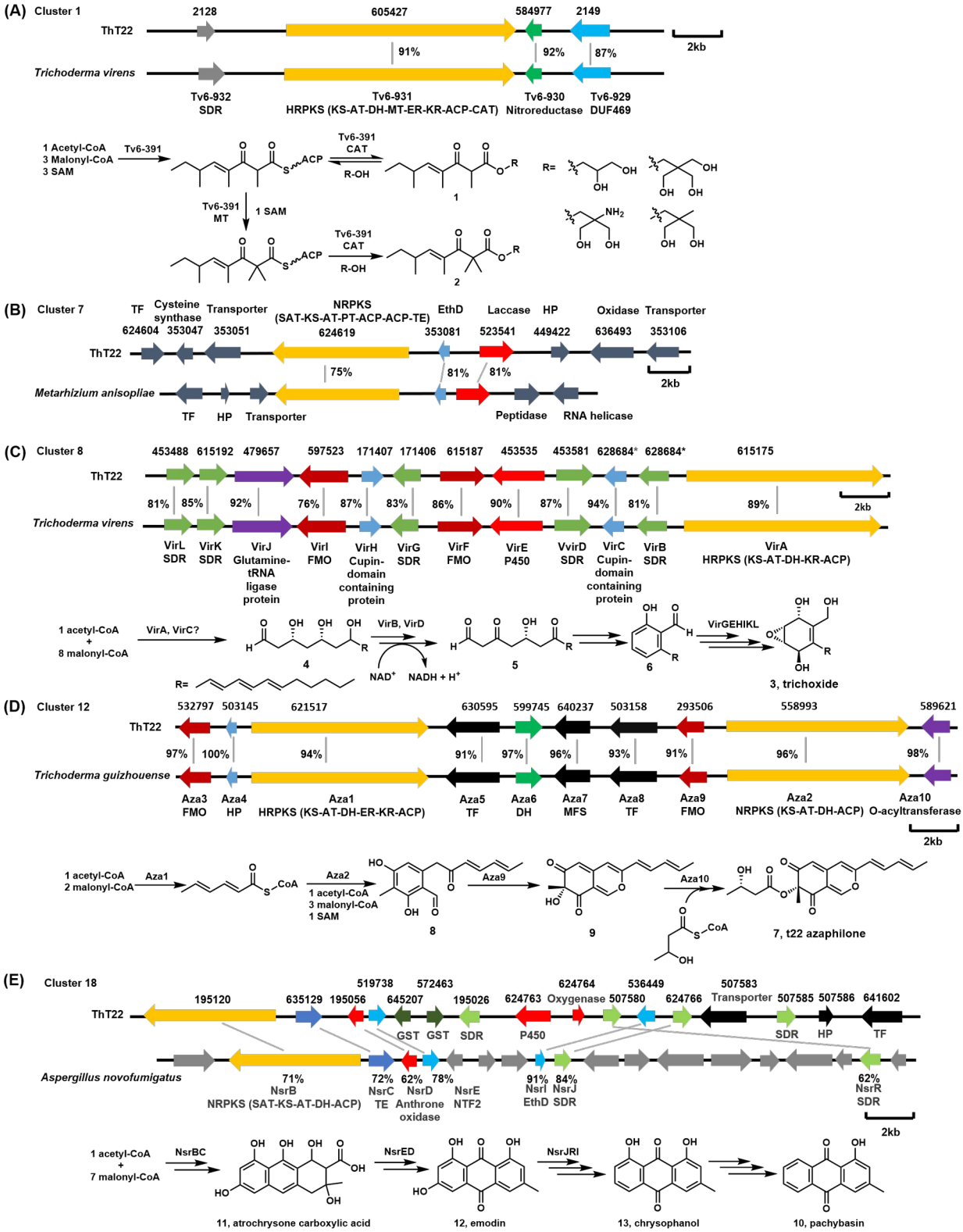
(A) Cluster 1
ThT22
2128
605427
584977
2149
2kb
91%
92%
87%
Trichoderma virens
Tv6-932 SDR
Tv6-931 HRPKS (KS-AT-DH-MT-ER-KR-ACP-CAT)
Tv6-930 Nitroreductase
Tv6-929 DUF469
1 Acetyl-CoA
3 Malonyl-CoA
3 SAM
Tv6-391
Tv6-391 CAT
R-OH
1
R=
Tv6-391 MT
1 SAM
2
(B) Cluster 7
TF
Cysteine synthase
Transporter
NRPKS (SAT-KS-AT-PT-ACP-ACP-TE)
EthD
Laccase
HP
Oxidase
Transporter
624604
353047
353051
624619
353081
523541
449422
636493
353106
75%
81%
81%
Metarhizium anisopliae
Peptidase
RNA helicase
(C) Cluster 8
453488
615192
479657
597523
171407
171406
615187
453535
453581
628684*
628684*
615175
81%
85%
92%
76%
87%
83%
86%
90%
87%
94%
81%
89%
Trichoderma virens
VirL SDR
VirK SDR
VirJ Glutamine-tRNA ligase protein
VirI FMO
VirH Cupin-domain containing protein
VirG SDR
VirF FMO
VirE P450
VvirD SDR
VirC Cupin-domain containing protein
VirB SDR
VirA HRPKS (KS-AT-DH-KR-ACP)
1 acetyl-CoA + 8 malonyl-CoA
VirA, VirC?
VirB, VirD
NAD+
NADH + H+
VirGEHIKL
4
5
6
3, trichoxide
(D) Cluster 12
532797
503145
621517
630595
599745
640237
503158
293506
558993
589621
97%
100%
94%
91%
97%
96%
93%
91%
96%
98%
Trichoderma guizhouense
Aza3 FMO
Aza4 HP
Aza1 HRPKS (KS-AT-DH-ER-KR-ACP)
Aza5 TF
Aza6 DH
Aza7 MFS
Aza8 TF
Aza9 FMO
Aza2 NRPKS (KS-AT-DH-ACP)
Aza10 O-acyltransferase
1 acetyl-CoA
2 malonyl-CoA
Aza1
Aza2
1 acetyl-CoA
3 malonyl-CoA
1 SAM
Aza9
Aza10
8
9
7, t22 azaphilone
(E) Cluster 18
519738
572463
624764
536449
507583
195120
635129
195056
645207
195026
624763
Oxygenase
507580
624766
Transporter
507585
507586
641602
GST
GST
SDR
P450
SDR
HP
TF
Aspergillus novofumigatus
71% NsrB NRPKS (SAT-KS-AT-DH-ACP)
72% NsrC TE
62% NsrD Anthrone oxidase
78% NsrE NTF2
91% NsrI EthD
84% NsrJ SDR
62% NsrR SDR
2kb
1 acetyl-CoA + 7 malonyl-CoA
NsrBC
NsrED
NsrJRI
11, atrochrysone carboxylic acid
12, emodin
13, chrysophanol
10, pachybasin

Figure 3

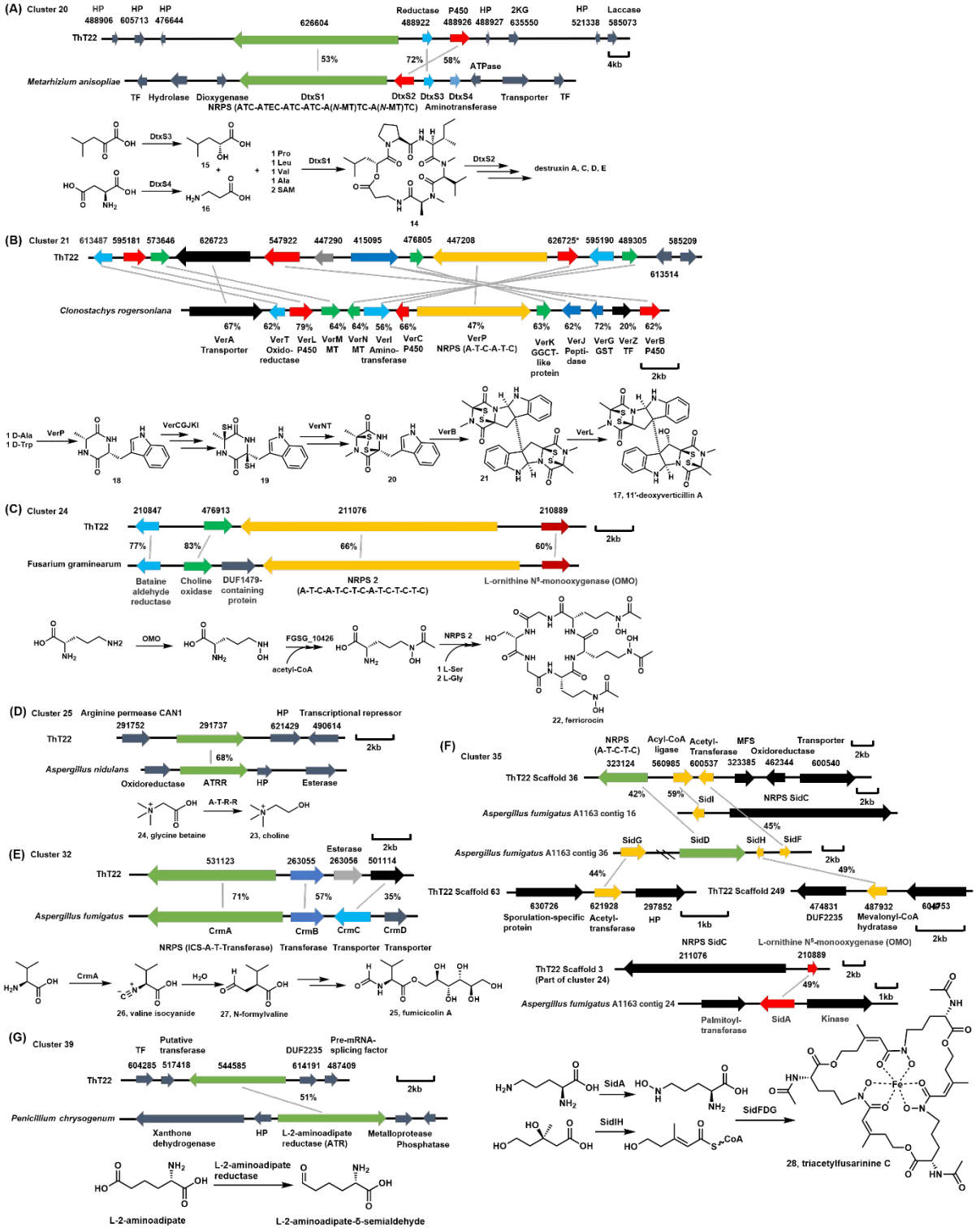
(A) Cluster 20
HP 488906
HP 605713
HP 476644
626604
Reductase 488922
P450 488926
HP 488927
2KG 635550
HP 521338
Laccase 585073
ThT22
53%
72%
58%
ATPase
4kb
Metarhizium anisopliae
TF
Hydrolase
Dioxygenase
DtxS1
DtxS2
DtxS3
DtxS4
Transporter
TF
NRPS (ATC-ATEC-ATC-ATC-A(N-MT)TC-A(N-MT)TC)
Aminotransferase
DtxS3
DtxS4
15
16
1 Pro
1 Leu
1 Val
1 Ala
2 SAM
DtxS1
DtxS2
destruxin A, C, D, E
14
(B) Cluster 21
613487
595181
573646
626723
547922
447290
415095
476805
447208
626725*
595190
489305
585209
613514
ThT22
Clonostachys rogersoniana
67% VerA Transporter
62% VerT Oxido-reductase
79% VerL P450
64% VerM MT
64% VerN MT
56% VerI Amino-transferase
66% VerC P450
47% VerP NRPS (A-T-C-A-T-C)
63% VerK GGCT-like protein
62% VerJ Pepti-dase
72% VerG GST
20% VerZ TF
62% VerB P450
2kb
1 D-Ala
1 D-Trp
VerP
VerCGJKI
VerNT
VerB
VerL
18
19
20
21
17, 11'-deoxyverticillin A
(C) Cluster 24
210847
476913
211076
210889
ThT22
2kb
77%
83%
66%
60%
Fusarium graminearum
Bataine aldehyde reductase
Choline oxidase
DUF1479-containing protein
NRPS 2 (A-T-C-A-T-C-T-C-A-T-C-T-C-T-C)
L-ornithine N5-monooxygenase (OMO)
OMO
FGSG_10426
acetyl-CoA
NRPS 2
1 L-Ser
2 L-Gly
22, ferricrocin
(D) Cluster 25
Arginine permease CAN1
291752
291737
HP 621429
Transcriptional repressor 490614
ThT22
2kb
68%
Aspergillus nidulans
Oxidoreductase
ATRR
HP
Esterase
A-T-R-R
24, glycine betaine
23, choline
(E) Cluster 32
531123
263055
Esterase 263056
501114
2kb
ThT22
71%
57%
35%
Aspergillus fumigatus
CrmA
CrmB
CrmC
CrmD
NRPS (ICS-A-T-Transferase)
Transferase
Transporter
Transporter
CrmA
H2O
26, valine isocyanide
27, N-formylvaline
25, fumicicolin A
(F) Cluster 35
NRPS (A-T-C-T-C) 323124
Acyl-CoA ligase 560985
Acetyl-Transferase 600537
MFS 323385
Oxidoreductase 462344
Transporter 600540
2kb
ThT22 Scaffold 36
42%
59%
SidI
NRPS SidC
2kb
Aspergillus fumigatus A1163 contig 16
45%
Aspergillus fumigatus A1163 contig 36
SidG
SidD
SidH
SidF
2kb
44%
49%
ThT22 Scaffold 63
ThT22 Scaffold 249
630726 Sporulation-specific protein
621928 Acetyl-transferase
297852 HP
1kb
474831 DUF2235
487932 Mevalonyl-CoA hydratase
604753
2kb
NRPS SidC
L-ornithine N5-monooxygenase (OMO)
211076
210889
2kb
ThT22 Scaffold 3 (Part of cluster 24)
49%
1kb
Aspergillus fumigatus A1163 contig 24
Palmitoyl-transferase
SidA
Kinase
(G) Cluster 39
TF 604285
Putative transferase 517418
544585
DUF2235 614191
Pre-mRNA-splicing factor 487409
ThT22
2kb
51%
Penicillium chrysogenum
Xanthone dehydrogenase
HP
L-2-aminoadipate reductase (ATR)
Metalloprotease
Phosphatase
L-2-aminoadipate reductase
L-2-aminoadipate
L-2-aminoadipate-δ-semialdehyde
SidA
SidIH
SidFDG
28, triacetylfusarinine C

Figure 4

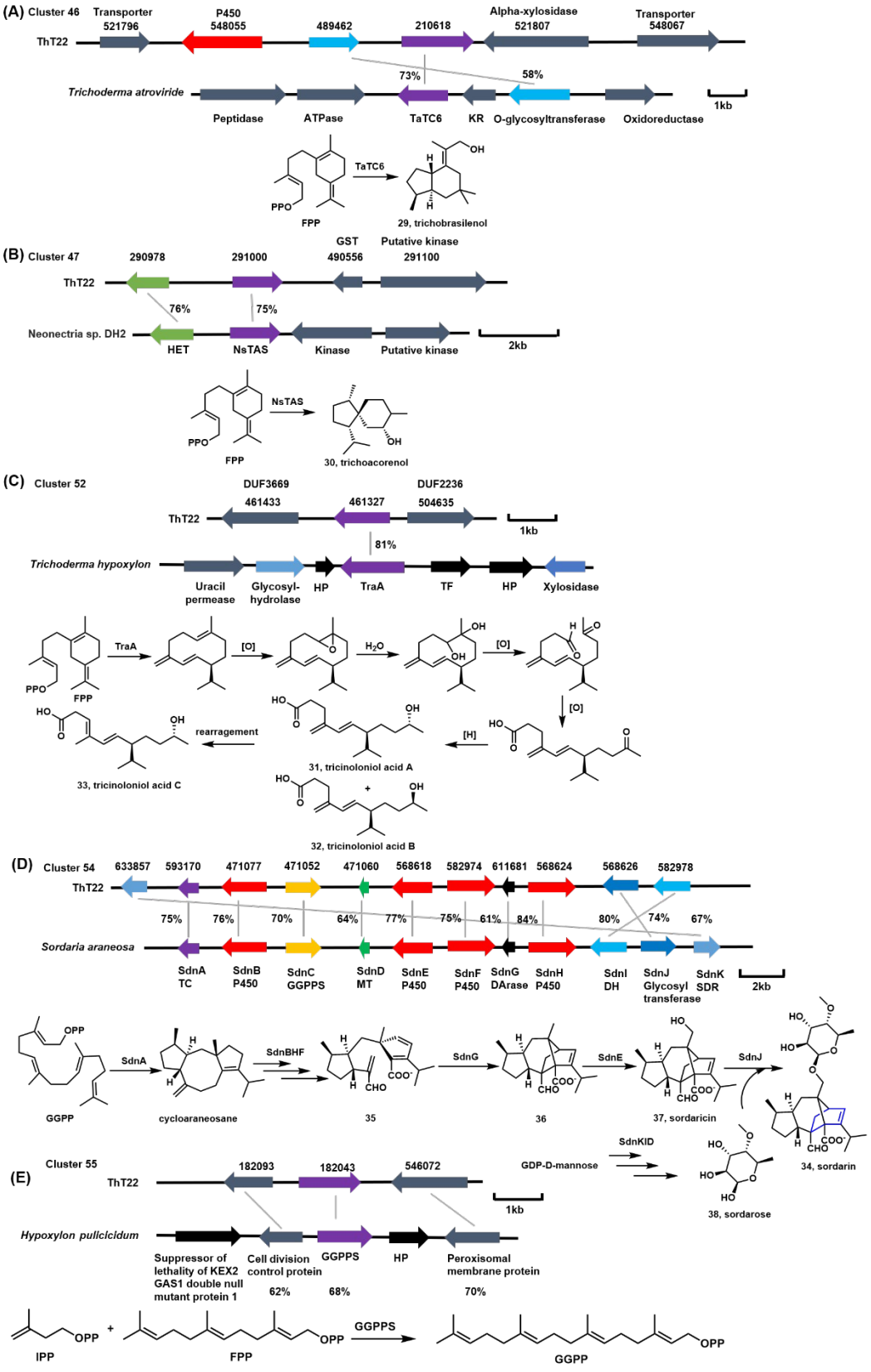
(A) Cluster 46
Transporter 521796
P450 548055
489462
210618
Alpha-xylosidase 521807
Transporter 548067
ThT22
73%
58%
Trichoderma atroviride
1kb
Peptidase
ATPase
TaTC6
KR
O-glycosyltransferase
Oxidoreductase
TaTC6
PPO
FPP
29, trichobrasilenol
(B) Cluster 47
290978
291000
GST 490556
Putative kinase 291100
ThT22
76%
75%
Neonectria sp. DH2
2kb
HET
NsTAS
Kinase
Putative kinase
NsTAS
PPO
FPP
30, trichoacorenol
(C) Cluster 52
DUF3669 461433
461327
DUF2236 504635
ThT22
1kb
81%
Trichoderma hypoxylon
Uracil permease
Glycosyl-hydrolase
HP
TraA
TF
HP
Xylosidase
TraA
PPO
FPP
[O]
H2O
[O]
[O]
[H]
rearragement
33, tricinoloniol acid C
31, tricinoloniol acid A
32, tricinoloniol acid B
(D) Cluster 54
633857 593170 471077 471052 471060 568618 582974 611681 568624 568626 582978
ThT22
75% 76% 70% 64% 77% 75% 61% 84% 80% 74% 67%
Sordaria araneosa
SdnA TC
SdnB P450
SdnC GGPPS
SdnD MT
SdnE P450
SdnF P450
SdnG DArase
SdnH P450
SdnI DH
SdnJ Glycosyl transferase
SdnK SDR
2kb
OPP
SdnA
SdnBHF
SdnG
SdnE
SdnJ
GGPP
cycloaraneosane
35
36
37, sordaricin
34, sordarin
(E) Cluster 55
182093
182043
546072
ThT22
1kb
Hypoxylon pulicicidum
Suppressor of lethality of KEX2 GAS1 double null mutant protein 1
Cell division control protein
GGPPS
HP
Peroxisomal membrane protein
62%
68%
70%
GDP-D-mannose
SdnKID
38, sordarose
IPP
OPP
FPP
GGPPS
GGPP

Figure 5

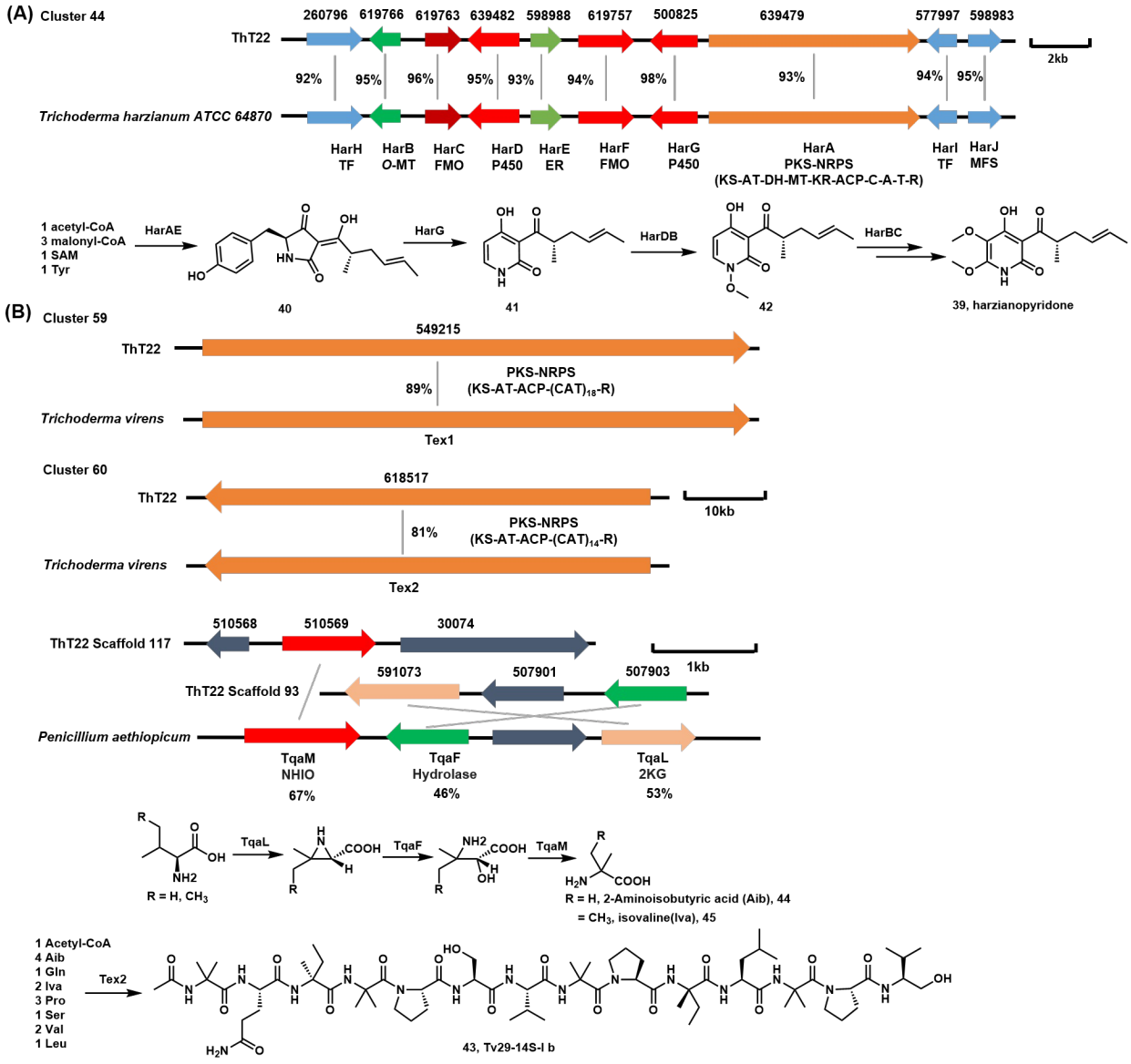
(A) Cluster 44
260796 619766 619763 639482 598988 619757 500825 639479 577997 598983
ThT22
2kb
92% 95% 96% 95% 93% 94% 98% 93% 94% 95%
Trichoderma harzianum ATCC 64870
HarH TF
HarB O-MT
HarC FMO
HarD P450
HarE ER
HarF FMO
HarG P450
HarA PKS-NRPS (KS-AT-DH-MT-KR-ACP-C-A-T-R)
HarI TF
HarJ MFS
1 acetyl-CoA
3 malonyl-CoA
1 SAM
1 Tyr
HarAE
HarG
HarDB
HarBC
40
41
42
39, harzianopyridone
(B) Cluster 59
549215
ThT22
89%
PKS-NRPS (KS-AT-ACP-(CAT)18-R)
Trichoderma virens
Tex1
Cluster 60
618517
ThT22
10kb
81%
PKS-NRPS (KS-AT-ACP-(CAT)14-R)
Trichoderma virens
Tex2
510568 510569 30074
ThT22 Scaffold 117
1kb
591073 507901 507903
ThT22 Scaffold 93
Penicillium aethiopicum
TqaM NHIO 67%
TqaF Hydrolase 46%
TqaL 2KG 53%
TqaL
TqaF
TqaM
R = H, CH3
R = H, 2-Aminoisobutyric acid (Aib), 44
= CH3, isovaline(Iva), 45
1 Acetyl-CoA
4 Aib
1 Gln
2 Iva
3 Pro
1 Ser
2 Val
1 Leu
Tex2
43, Tv29-14S-I b

Figure 6

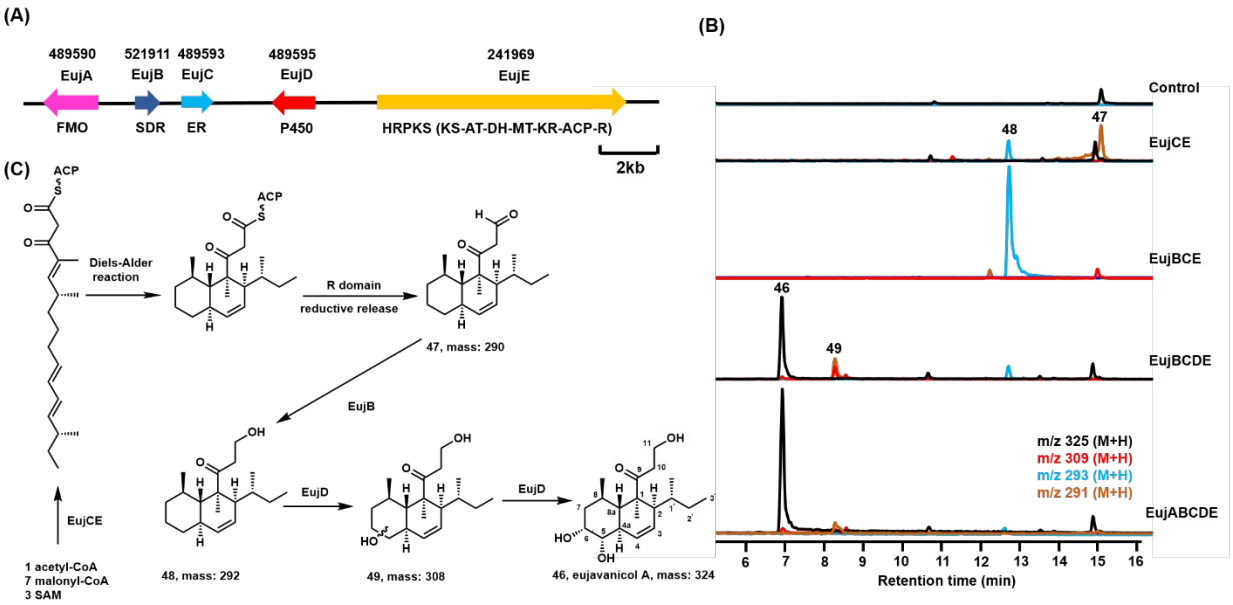
(A)
489590
EujA
521911
EujB
489593
EujC
489595
EujD
241969
EujE
FMO
SDR
ER
P450
HRPKS (KS-AT-DH-MT-KR-ACP-R)
2kb
(B)
Control
EujCE
EujBCE
EujBCDE
EujABCDE
47
48
46
49
m/z 325 (M+H)
m/z 309 (M+H)
m/z 293 (M+H)
m/z 291 (M+H)
Retention time (min)
(C)
ACP
Diels-Alder reaction
R domain reductive release
47, mass: 290
EujB
EujD
EujD
EujCE
1 acetyl-CoA
7 malonyl-CoA
3 SAM
48, mass: 292
49, mass: 308
46, eujavanicol A, mass: 324

Figure 7

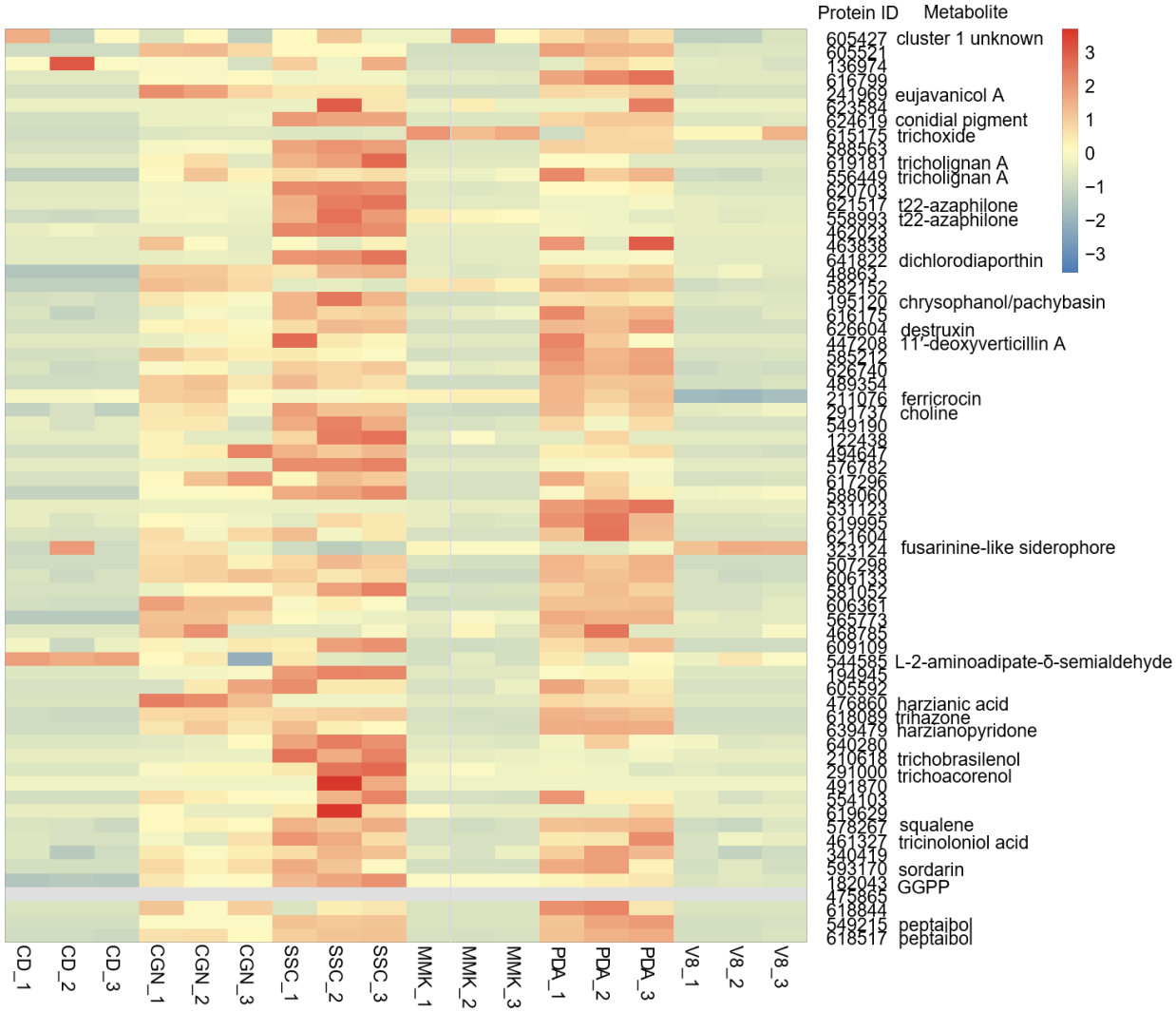
Protein ID
Metabolite
605427 cluster 1 unknown
605521
136974
616799
241969 eujavanicol A
623584
624619 conidial pigment
615175 trichoxide
588563
619181 tricholignan A
556449 tricholignan A
620703
621517 t22-azaphilone
558993 t22-azaphilone
462023
463838
641822 dichlorodiaporthin
48863
582152
195120 chrysophanol/pachybasin
616175
626604 destruxin
447208 11'-deoxyverticillin A
585211
626740
468354
211076 ferricrocin
291737 choline
549190
122438
494647
576782
617296
588060
531123
619995
621604
323124 fusarinine-like siderophore
507298
606133
581052
606361
565773
468785
609109
544585 L-2-aminoadipate-δ-semialdehyde
194945
605592
476865 harzianic acid
618089 trihazone
639479 harzianopyridone
640290
210618 trichobrasilenol
291000 trichoacorenol
491870
554103
619629
578267 squalene
461327 tricinoloniol acid
340419
593170 sordarin
182043 GGPP
475865
618844
549215 peptaibol
618517 peptaibol
3
2
1
0
−1
−2
−3
CD_1
CD_2
CD_3
CGN_1
CGN_2
CGN_3
SSC_1
SSC_2
SSC_3
MMK_1
MMK_2
MMK_3
PDA_1
PDA_2
PDA_3
V8_1
V8_2
V8_3

Figure 8

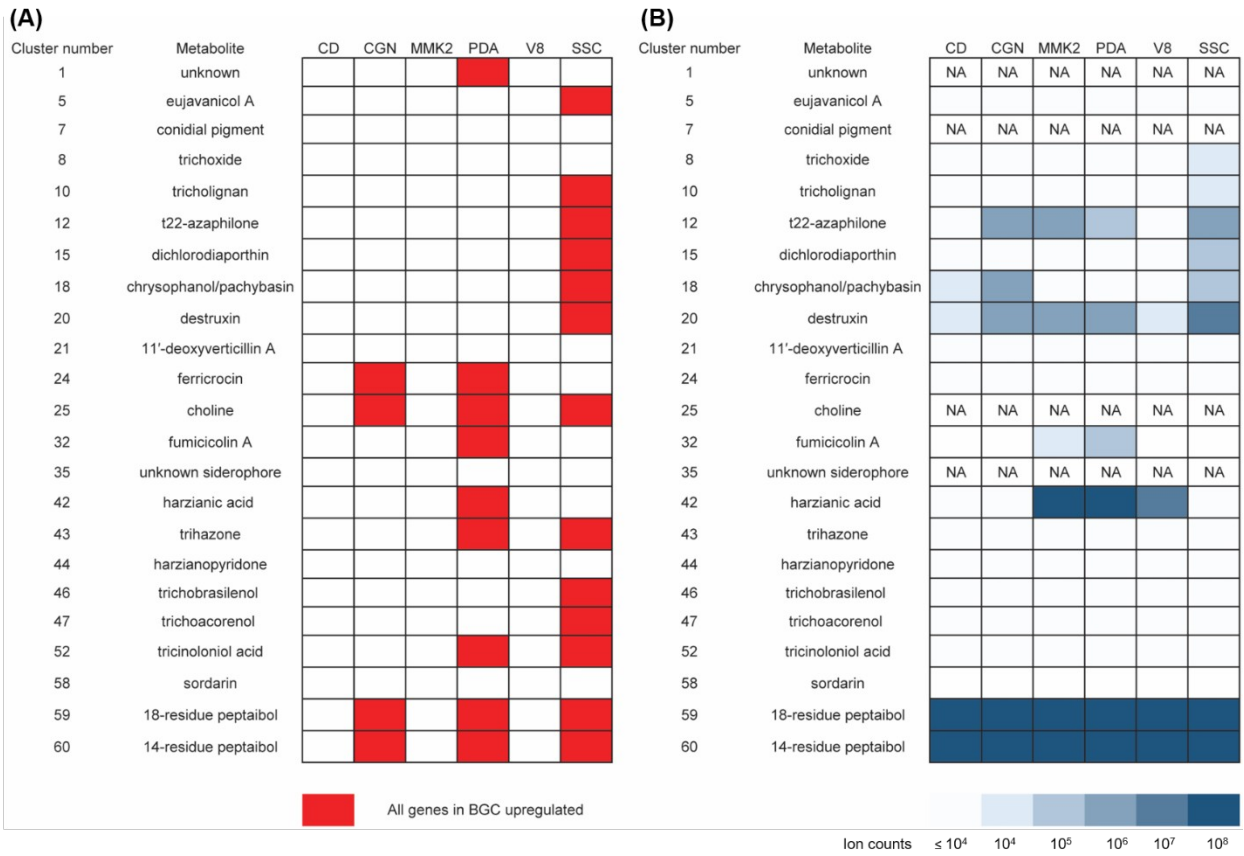
(A)
Cluster number
Metabolite
CD
CGN
MMK2
PDA
V8
SSC
1 unknown
5 eujavanicol A
7 conidial pigment
8 trichoxide
10 tricholignan
12 t22-azaphilone
15 dichlorodiaporthin
18 chrysophanol/pachybasin
20 destruxin
21 11′-deoxyverticillin A
24 ferricrocin
25 choline
32 fumicicolin A
35 unknown siderophore
42 harzianic acid
43 trihazone
44 harzianopyridone
46 trichobrasilenol
47 trichoacorenol
52 tricinoloniol acid
58 sordarin
59 18-residue peptaibol
60 14-residue peptaibol
All genes in BGC upregulated
(B)
Cluster number
Metabolite
CD
CGN
MMK2
PDA
V8
SSC
NA
Ion counts
≤ 10⁴
10⁴
10⁵
10⁶
10⁷
10⁸

Figure 9

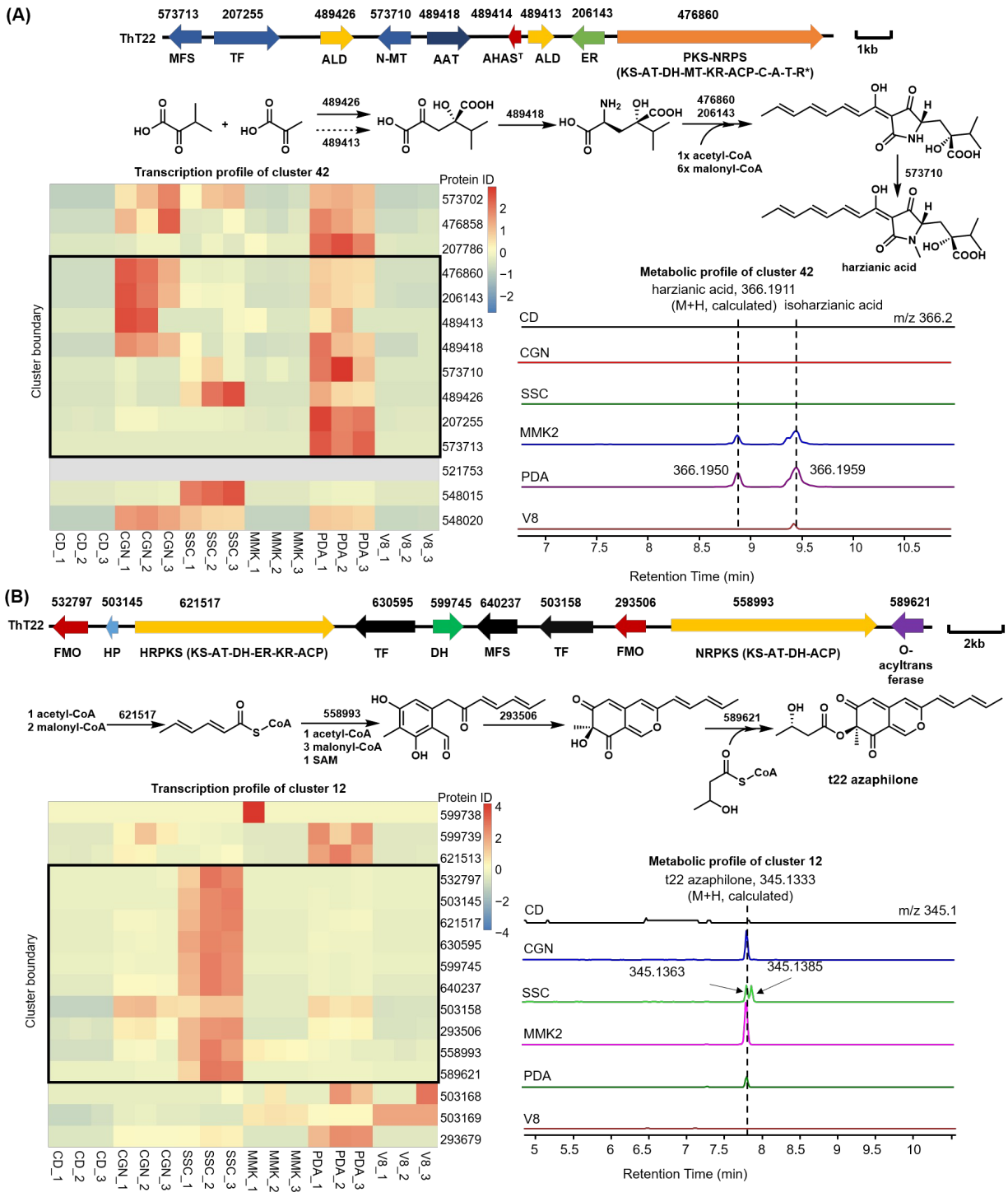
(A)
ThT22
573713 207255 489426 573710 489418 489414 489413 206143 476860
MFS TF ALD N-MT AAT AHAS^T ALD ER PKS-NRPS (KS-AT-DH-MT-KR-ACP-C-A-T-R*)
1kb
489426
489413
489418
476860
206143
1x acetyl-CoA
6x malonyl-CoA
573710
harzianic acid
Transcription profile of cluster 42
Protein ID
573702
476858
207786
476860
206143
489413
489418
573710
489426
207255
573713
521753
548015
548020
Cluster boundary
CD_1 CD_2 CD_3 CGN_1 CGN_2 CGN_3 SSC_1 SSC_2 SSC_3 MMK_1 MMK_2 MMK_3 PDA_1 PDA_2 PDA_3 V8_1 V8_2 V8_3
Metabolic profile of cluster 42
harzianic acid, 366.1911
(M+H, calculated) isoharzianic acid
CD
CGN
SSC
MMK2
PDA
V8
m/z 366.2
366.1950
366.1959
Retention Time (min)
(B)
ThT22
532797 503145 621517 630595 599745 640237 503158 293506 558993 589621
FMO HP HRPKS (KS-AT-DH-ER-KR-ACP) TF DH MFS TF FMO NRPKS (KS-AT-DH-ACP) O-acyltransferase
2kb
1 acetyl-CoA
2 malonyl-CoA
621517
558993
1 acetyl-CoA
3 malonyl-CoA
1 SAM
293506
589621
t22 azaphilone
Transcription profile of cluster 12
Protein ID
599738
599739
621513
532797
503145
621517
630595
599745
640237
503158
293506
558993
589621
503168
503169
293679
Cluster boundary
CD_1 CD_2 CD_3 CGN_1 CGN_2 CGN_3 SSC_1 SSC_2 SSC_3 MMK_1 MMK_2 MMK_3 PDA_1 PDA_2 PDA_3 V8_1 V8_2 V8_3
Metabolic profile of cluster 12
t22 azaphilone, 345.1333
(M+H, calculated)
CD
CGN
SSC
MMK2
PDA
V8
m/z 345.1
345.1363
345.1385
Retention Time (min)

841

TOC GRAPHIC

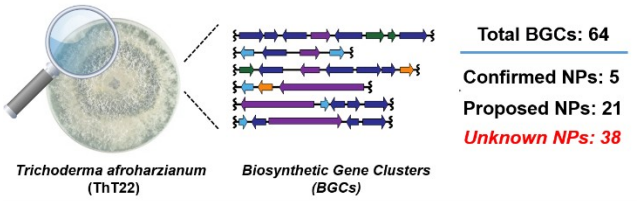
Total BGCs: 64
Confirmed NPs: 5
Proposed NPs: 21
Unknown NPs: 38
Trichoderma afroharzianum
(ThT22)
Biosynthetic Gene Clusters
(BGCs)